One main goal of this study was to examine the ability of AAV8 to transfer foreign genes into identified neuronal cell types in primate brain. Specifically, we explored the ability of AAV8 to transfect projection neurons in the striatum and dopaminergic neurons in the substantia nigra, which constitute functional circuits within the nigrostriatal loop [10–13]. Clinically, dysfunctions of the basal ganglia circuit have been related to many neurological disorders including Parkinson's disease and Huntington's disease. AAV-mediated gene transfer is one of the most promising means for gene therapy of these diseases, and preclinical investigations of the tropism of AAV for functionally identified neurons are requisite steps for future practical applications. In this study, we successfully showed efficient AAV8 transfection of calbindin-positive neurons in the striatum and TH-positive dopaminergic neurons in the substantia nigra. These results indicate the potential of AAV8 vector as a therapeutic tool for basal ganglia-related diseases. Other than the therapeutic applications, AAV8 will be useful to deliver molecular tools to experimentally monitor or manipulate neuronal activities in primate brains [3,4]. Further research is needed to clarify the infection spectrum of AAV8 and other AAV serotypes in many other neuronal cell types in the primate brain.

Conclusion

AAV8 vector has strong tropism for neurons but not for glia in the brain of the common marmoset *in vivo*. Efficient AAV8-mediated gene transfer into identified neuronal cell types, calbindin-positive medium spiny neurons in the striatum and TH-positive dopaminergic neurons in the substantia nigra, was also successfully shown.

Acknowledgements

This work was supported by a JSPS Research Fellowship for Young Scientists (Y.M.), and by PRESTO, JST (K.N.). All the authors declare that they have no conflict of interest.

References

1 Daya S, Berns KI. Gene therapy using adeno-associated virus vectors. *Clin Microbiol Rev* 2008; **21**:583–593.
2 Kaplitt MG, Leone P, Samulski RJ, Xiao X, Pfaff DW, O'Malley KL, *et al.* Long-term gene expression and phenotypic correction using adeno-associated virus vectors in the mammalian brain. *Nat Genet* 1994; **8**:148–154.
3 Zhang F, Aravanis AM, Adamantidis A, de Lecea L, Deisseroth K. Circuit-breakers: optical technologies for probing neural signals and systems. *Nat Rev Neurosci* 2007; **8**:577–581.
4 Han X, Qian X, Bernstein JG, Zhou HH, Franzesi GT, Stern P, *et al.* Millisecond-timescale optical control of neural dynamics in the nonhuman primate brain. *Neuron* 2009; **62**:191–198.
5 Ohshima S, Shin JH, Yuasa K, Nishiyama A, Kira J, Okada T, *et al.* Transduction efficiency and immune response associated with the administration of AAV8 vector into dog skeletal muscle. *Mol Ther* 2009; **17**:73–80.
6 Zincarelli C, Soltys S, Rengo G, Rabinowitz JE. Analysis of AAV serotypes 1-9 mediated gene expression and tropism in mice after systemic injection. *Mol Ther* 2008; **16**:1073–1080.
7 Gao GP, Alvira MR, Wang L, Calcedo R, Johnston J, Wilson JM. Novel adeno-associated viruses from rhesus monkeys as vectors for human gene therapy. *Proc Natl Acad Sci U S A* 2002; **99**:11854–11859.
8 Rutledge EA, Halbert CL, Russell DW. Infectious clones and vectors derived from adeno-associated virus (AAV) serotypes other than AAV type 2. *J Virol* 1998; **72**:309–319.
9 Broekman ML, Comer LA, Hyman BT, Sena-Esteves M. Adeno-associated virus vectors serotyped with AAV8 capsid are more efficient than AAV-1 or -2 serotypes for widespread gene delivery to the neonatal mouse brain. *Neuroscience* 2006; **138**:501–510.
10 Nicola SM, Surmeier J, Malenka RC. Dopaminergic modulation of neuronal excitability in the striatum and nucleus accumbens. *Annu Rev Neurosci* 2000; **23**:185–215.
11 Nambu A, Tokuno H, Takada M. Functional significance of the cortico-subthalamo-pallidal, hyperdirect, pathway. *Neurosci Res* 2002; **43**:111–117.
12 Redgrave P, Gurney K. The short-latency dopamine signal: a role in discovering novel actions? *Nat Rev Neurosci* 2006; **7**:967–975.
13 Obeso JA, Marin C, Rodriguez-Oroz C, Blesa J, Benitez-Temino B, Mena-Segovia J, *et al.* The basal ganglia in Parkinson's disease: current concepts and unexplained observations. *Ann Neurol* 2008; **64 (Suppl 2)**:S30–S46.
14 Okada T, Nonaka-Sarukawa M, Uchibori R, Kinoshita K, Hayashita-Kinoh H, Nitahara-Kasahara Y, *et al.* Scalable purification of adeno-associated virus serotype 1 (AAV1) and AAV8 vectors, using dual ion-exchange adsorptive membranes. *Hum Gene Ther* 2009; **20**:1013–1021.
15 Okada T, Nomoto T, Yoshioka T, Nonaka-Sarukawa M, Ito T, Ogura T, *et al.* Large-scale production of recombinant viruses by use of a large culture vessel with active gassing. *Hum Gene Ther* 2005; **16**:1212–1218.
16 Matsushita T, Elliger S, Elliger C, Podsakoff G, Villarreal L, Kurtzman GJ, *et al.* Adeno-associated virus vectors can be efficiently produced without helper virus. *Gene Ther* 1998; **5**:938–945.
17 Okada T, Shimazaki K, Nomoto T, Matsushita T, Mizukami H, Urabe M, *et al.* Adeno-associated viral vector-mediated gene therapy of ischemia-induced neuronal death. *Methods Enzymol* 2002; **346**:378–393.
18 Burman KJ, Palmer SM, Gamberini M, Spitzer MW, Rosa MG. Anatomical and physiological definition of the motor cortex of the marmoset monkey. *J Comp Neurol* 2008; **506**:860–876.
19 Eslamboli A, Georgievska B, Ridley RM, Baker HF, Muzyczka N, Burger C, *et al.* Continuous low-level glial cell line-derived neurotrophic factor delivery using recombinant adeno-associated viral vectors provides neuroprotection and induces behavioral recovery in a primate model of Parkinson's disease. *J Neurosci* 2005; **25**:769–777.
20 Eslamboli A, Romero-Ramos M, Burger C, Bjorklund T, Muzyczka N, Mandel RJ, *et al.* Long-term consequences of human alpha-synuclein overexpression in the primate ventral midbrain. *Brain* 2007; **130**:799–815.
21 Nakahira E, Yuasa S. Neuronal generation, migration, and differentiation in the mouse hippocampal primordium as revealed by enhanced green fluorescent protein gene transfer by means of in utero electroporation. *J Comp Neurol* 2005; **483**:329–340.
22 Bourne JA, Warner CE, Rosa MG. Topographic and laminar maturation of striate cortex in early postnatal marmoset monkeys, as revealed by neurofilament immunohistochemistry. *Cereb Cortex* 2005; **15**:740–748.
23 Parent A, Fortin M, Cote PY, Cicchetti F. Calcium-binding proteins in primate basal ganglia. *Neurosci Res* 1996; **25**:309–334.
24 Dodiya HB, Bjorklund T, Stansell III J, Mandel RJ, Kirik D, Kordower JH. Differential transduction following basal ganglia administration of distinct pseudotyped AAV capsid serotypes in nonhuman primates. *Mol Ther* 2009; doi:10.1038/mt.2009.216.
25 Klein RL, Dayton RD, Leidenheimer NJ, Jansen K, Golde TE, Zweig RM. Efficient neuronal gene transfer with AAV8 leads to neurotoxic levels of tau or green fluorescent proteins. *Mol Ther* 2006; **13**:517–527.

EXPERIMENTAL CELL RESEARCH 316 (2010) 2932–2944

available at www.sciencedirect.com

ScienceDirect

www.elsevier.com/locate/yexcr

Research Article

Six family genes control the proliferation and differentiation of muscle satellite cells

Hiroshi Yajima[a], *Norio Motohashi*[b], *Yusuke Ono*[b], *Shigeru Sato*[a], *Keiko Ikeda*[a], *Satoru Masuda*[b], *Erica Yada*[b], *Hironori Kanesaki*[b], *Yuko Miyagoe-Suzuki*[b], *Shin'ichi Takeda*[b], *Kiyoshi Kawakami*[a,*]

[a]*Division of Biology, Center for Molecular Medicine, Jichi Medical University, Tochigi, Japan*
[b]*Department of Molecular Therapy, National Institute of Neuroscience, National Center of Neurology and Psychiatry, Tokyo, Japan*

ARTICLE INFORMATION

Article Chronology:
Received 1 April 2010
Revised version received 19 July 2010
Accepted 3 August 2010
Available online 6 August 2010

Keywords:
Muscle satellite cell
Six gene
Cell proliferation
Muscle differentiation
Retrovirus-mediated overexpression
Gene knockdown

ABSTRACT

Muscle satellite cells are essential for muscle growth and regeneration and their morphology, behavior and gene expression have been extensively studied. However, the mechanisms involved in their proliferation and differentiation remain elusive. Six1 and Six4 proteins were expressed in the nuclei of myofibers of adult mice and the numbers of myoblasts positive for Six1 and Six4 increased during regeneration of skeletal muscles. Six1 and Six4 were expressed in quiescent, activated and differentiated muscle satellite cells isolated from adult skeletal muscle. Overexpression of *Six4* and *Six5* repressed the proliferation and differentiation of satellite cells. Conversely, knockdown of Six5 resulted in augmented proliferation, and that of Six4 inhibited differentiation. Muscle satellite cells isolated from $Six4^{+/-}Six5^{-/-}$ mice proliferated to higher cell density though their differentiation was not altered. Meanwhile, overproduction of Six1 repressed proliferation and promoted differentiation of satellite cells. In addition, Six4 and Six5 repressed, while Six1 activated *myogenin* expression, suggesting that the differential regulation of *myogenin* expression is responsible for the differential effects of *Six* genes. The results indicated the involvement of *Six* genes in the behavior of satellite cells and identified *Six* genes as potential target for manipulation of proliferation and differentiation of muscle satellite cells for therapeutic applications.

Introduction

Muscle satellite cells are tissue-specific stem cells that reside beneath the basal lamina surrounding the myofibers of mature adult skeletal muscles and play a major role in post-natal muscle growth and regeneration [1, for review see 2]. In the intact adult muscles, satellite cells are mitotically quiescent, while in the injured or damaged muscle, they are activated to proliferate, differentiate and then regenerate myofibers by fusing with each other or with residual fibers. The recent discovery of specific markers for muscle satellite cells, including Pax7, M-cadherin, MyoD and myogenin, has allowed the identification of the status of these cells [2]. Pax7 and M-cadherin is expressed in quiescent satellite cells, while MyoD is rapidly induced during activation of satellite cells [3]. The Pax7- and MyoD-double-positive cells are regarded as transit amplifying cells and future myoblasts [3]. It is

* *Corresponding author.* Division of Biology, Center for Molecular Medicine, Jichi Medical University, 3311-1, Yakushiji, Shimotsuke, Tochigi, 329-0498, Japan. Fax: +81 285 44 5476.
E-mail address: kkawakam@jichi.ac.jp (K. Kawakami).

0014-4827/$ – see front matter © 2010 Elsevier Inc. All rights reserved.
doi:10.1016/j.yexcr.2010.08.001

noted that some transit amplifying cells become MyoD-negative, and those are thought to re-enter the quiescent state [3]. The expression of Pax7 is down-regulated before commitment to terminal differentiation. Despite such progress in our understanding of the lineage and behavior of muscle satellite cells, there are other areas that remain poorly understood; for example, the exact mechanism that orchestrates the proliferation and differentiation of these cells.

Recently, we developed a new and efficient method to isolate quiescent satellite cells using monoclonal antibody SM/C-2.6 [4]. SM/C-2.6-positive cells co-express M-cadherin and become MyoD-positive in growth media. They are differentiated into desmin- and MyoD-positive myofibers under differentiation conditions. In the same study, we showed that the sorted muscle satellite cells differentiated into muscle fibers following their injection into *mdx* mouse muscles [4]. Furthermore, genome-wide gene expression analysis using the isolated cells allowed the identification of a quiescent cell-specific marker, calcitonin receptor (CTR), implicating the involvement of calcitonin/CTR signaling in the activation of satellite cells [5]. Thus, the SM/C-2.6-positive satellite cells are useful tool for investigating the mechanism of regulation of proliferation and differentiation *in vitro* and allow us to gain a better understanding of the role of satellite cells during muscle regeneration, compared to the use of cell lines such as C2C12 and MM14 cells.

The *Six* genes have been identified as homologues of *Drosophila sine oculis*, which is crucial for compound-eye formation [6,7]. The mammalian *Six* gene family consists of six members, *Six1* to *Six6* [8]. During development, *Six1* and *Six4* play important roles in the formation of various organs, such as olfactory epithelium, cranial ganglia, inner ear, kidney, skeletal muscle and skeleton [9–20]. During skeletal muscle development, *Six1* and *Six4* are expressed in the somite and migrating myoblasts and play important roles in myogenesis [21–23]. Another member of the *Six* gene family, *Six5*, is expressed in the somite and adult skeletal muscles [22,24,25]. Genetic ablation of both *Six1* and *Six4* results in gross muscle hypoplasia [21]. Limb muscles derived from hypaxial progenitors disappear, as a result of aberrant migration and apoptosis of myoblasts, which are caused by down-regulation of Pax3. Epaxial and other hypaxial muscles are impaired through severely compromised expression of myogenic regulatory factors (MRF) genes, Mrf4 and myogenin, within the myotome [21]. Expression of myogenin is thought to be directly controlled by Six1, Six4 and Six5 via MEF3 sites *in vivo* [26] and in cultured cells [27]. Moreover, *Six1* and *Six4* are necessary for the induction of the fast-type-muscle program during myogenesis [23] and are involved in the assignment of the fast/glycolytic character of the myofiber in adult skeletal muscles [22]. However, there is virtually no information on the role of *Six1*, *Six4* and *Six5* in muscle regeneration, especially in the proliferation and differentiation of muscle satellite cells.

In the present study, we analyzed the expression of *Six1*, *Six4* and *Six5* in adult skeletal muscles during regeneration and in satellite cells *in vivo* and in culture. We examined the effects of overexpression and knockdown of *Six* genes on the proliferation and differentiation of isolated satellite cells *in vitro*. Finally, the proliferation and differentiation of muscle satellite cells isolated from *Six4*- and *Six5*-deficient mice were compared to those of wild-type mice. The results demonstrated the involvement of *Six* genes in the regulation of proliferation and differentiation of muscle satellite cells.

Results

Induction of expression of Six proteins during regeneration of adult skeletal muscle

To investigate the expression of *Six* genes during skeletal muscle regeneration, we induced muscle damage by injecting cardiotoxin into the tibialis anterior (TA) muscles of 8- to 12-week-old wild-type mice. Three days after the injection, transverse sections of TA muscles were prepared from the injected as well as intact mice and mapped the distribution of Six proteins by immunofluorescence using specific antibodies to Six1 and Six4 [10,18]. In the intact non-injected TA muscles, a considerable number of muscle nuclei was positive for Six1 (Fig. 1A). The Six1-positive nuclei were located inside the muscle basal laminae, which were visualized by immunofluorescence using anti-laminin antibody (Figs. 1B and C). This indicates that the nuclei of the myofibers are positive for Six1 in the adult skeletal muscle. Most of the Six1-positive nuclei were also positive for Six4 (Figs. 1D–F). In the regenerating TA muscle, the number of cells positive for Six1 was far greater than that of control TA muscle (Fig. 1I, compare to 1A). The Six1-positive cells in the regenerating TA muscle were located inside and outside the basal laminae (Figs. 1J and K). As observed in the control TA muscles, most of the cells positive for Six1 were also positive for Six4 in the regenerating TA muscle (Figs. 1L–N). It was noted that the relative intensities of immunofluorescent signals for Six1 and Six4 were more variable in the regenerating muscle (Fig. 1N), compared to those in the intact muscle (Fig. 1F). To determine the type of cells positive for Six1 and Six4, we examined the expression of MyoD, a marker of proliferating myogenic precursor cells and postmitotic myocytes in the regenerating muscle [28–30]. Triple immunofluorescence using anti-Six1, anti-Six4 and anti-MyoD antibodies revealed that most of the immunofluorescent signals of Six1 and Six4 were colocalized with that of MyoD (Figs. 1O and P). As shown in Fig. 1Q, $90.1 \pm 0.42\%$ of Six1-positive cells and $91.7 \pm 1.06\%$ of Six4-positive cells were colocalized with MyoD. Moreover, remarkable amounts of Six1 and Six4 immunofluorescent signals were positive for Ki67, a marker of proliferating cells, suggesting that substantial populations of Six1- and Six4-positive cells were mitotic (Figs. 1R–T, data not shown). Colocalization of Six1 and Six4 with MyoD was not observed in the control skeletal muscle (Figs. 1G and H). These findings indicate that (i) Six1 and Six4 are expressed both in normal and regenerating muscles and (ii) the number of cells positive for Six1 and Six4 robustly increases during regeneration of adult skeletal muscle and many of them are proliferating myogenic precursors.

Expression of Six proteins in muscle satellite cells

In the adult skeletal muscle, typical quiescent satellite cells can be recognized as mononuclear cells beneath the basal lamina, and these cells are positive for both Pax7 and M-cadherin [30–32]. To determine whether Six proteins are expressed in quiescent muscle satellite cells, we performed immunofluorescence studies for Six1, Pax7 and M-cadherin. Immunofluorescent signals of Pax7 (Fig. 2A) and M-cadherin (Fig. 2B) were observed in the mononuclear cells of adult TA muscle (Figs. 2A, B and E, arrowheads and insets). Six1 immunofluorescence signal was also observed in these cells

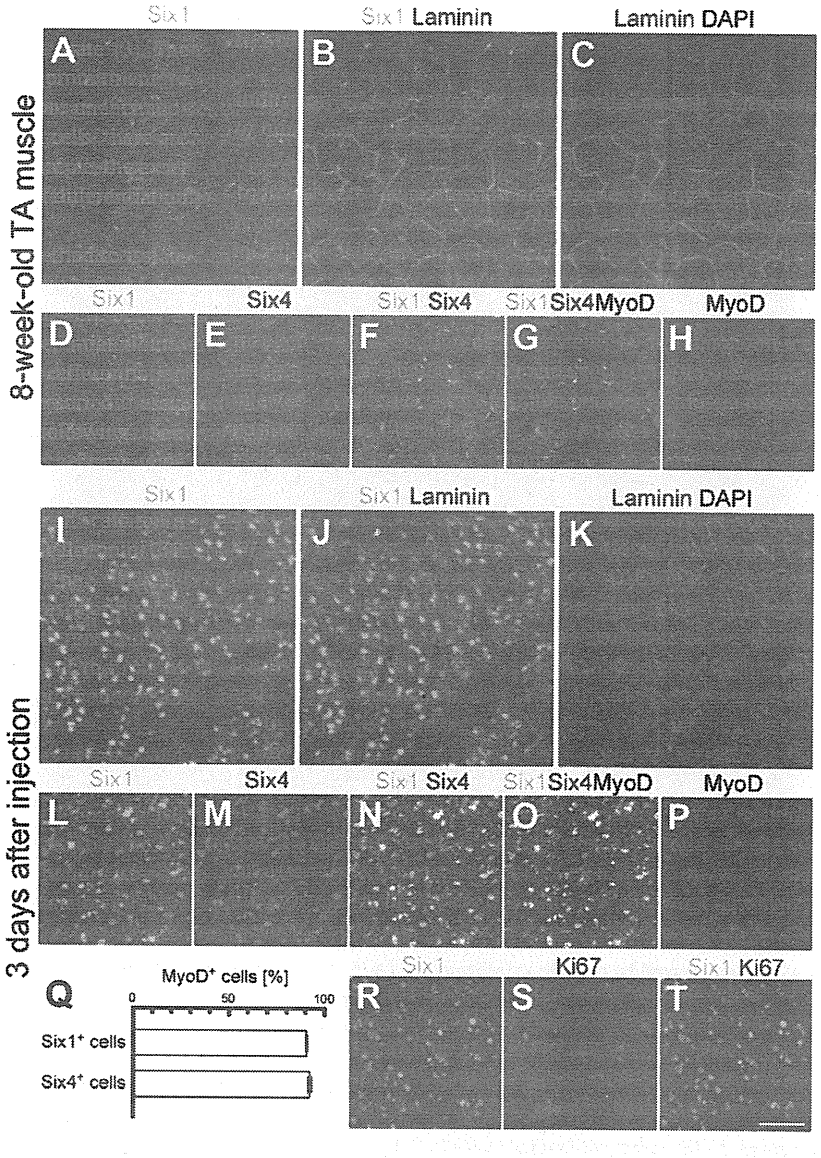

Fig. 1 – Expression of Six1 and Six4 in regenerating skeletal muscles of adult mice. (A–C) Cross-sections of intact TA muscle of 8-week-old mouse were stained with antibodies to Six1 (green) and laminin (red). Nuclei were stained with DAPI (blue). Note the subset of nuclei beneath the laminin layer is positive for Six1. (D–H) Immunofluorescence of cross-sections of TA muscle immunostained with antibodies for Six1 (green), Six4 (red) and MyoD (blue). Merged figures are shown in panels F and G. Most Six1-positive nuclei were positive for Six4 (E and F). MyoD was not detected in the adult TA muscle (H). (I–K) Cross-sections of regenerating TA muscle 3 days after cardiotoxin injection were co-immunostained with antibodies to Six1 (green) and laminin (red). Nuclei were stained with DAPI (blue). Note Six1-positive nuclei located inside and outside the laminin layer (J). (L–P) Immunofluorescence of cross-sections of regenerating TA muscle immunostained with antibodies for Six1 (green), Six4 (red) and MyoD (blue). Merged figures are shown in panels N and O. The majority of Six1-positive nuclei are also positive for Six4. Most of Six1- and Six4-positive nuclei are colocalized with MyoD. The percentages of MyoD-positive cells were quantified in (Q). Data are mean ± SEM. (R–T) Regenerating TA muscle immunostained with antibodies for Six1 (green) and Ki67 (red). A remarkable number of Six1-positive nuclei is positive for mitotic marker, Ki67. Scale bar: 50 μm.

(Figs. 2C and D, arrowheads and insets). The expression of Six4 was also observed in the satellite cells positive for M-cadherin in the adult TA muscle (Fig. 2F, thick arrow and inset). It is noteworthy that some of the nuclei within the myofibers, which were negative for Pax7 and M-cadherin, were positive for Six1 and Six4 (Figs. 2C–F arrows, data not shown). Vice versa, some of the Pax7 and M-cadherin-positive cells were negative for Six1 and Six4 (data not shown).

To examine the expression of Six proteins in muscle satellite cells during activation, proliferation and differentiation, we isolated and cultured satellite cells from limb and back muscles of wild-type mice by FACS technique using the monoclonal antibody SM/C-2.6 [4,5]

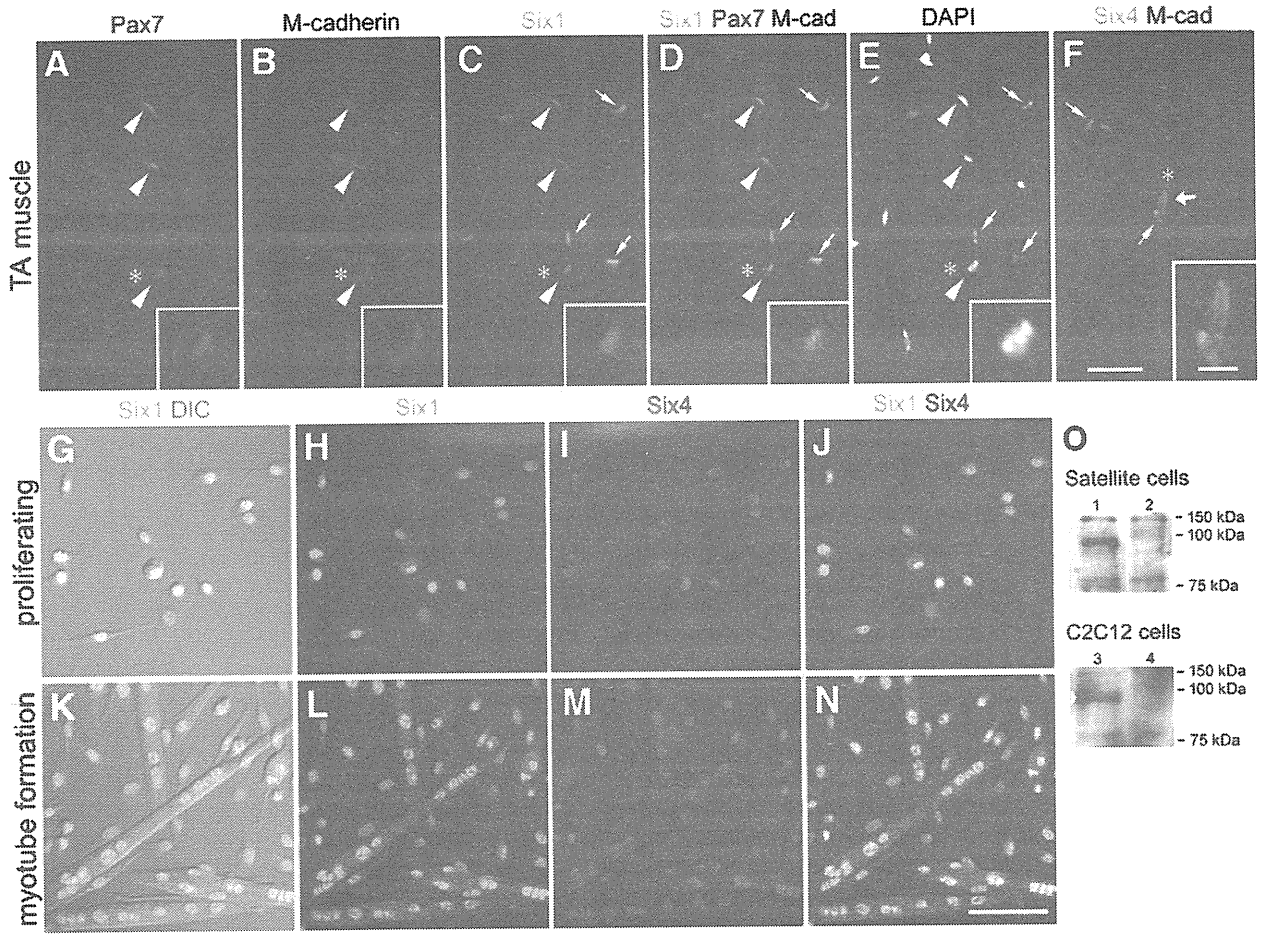

Fig. 2 – Six1, Six4 and Six5 are expressed in muscle satellite cells. (A–F) Cross-sections of TA muscle of 8-week-old mouse were immunostained with antibodies to Pax7 (red in A), M-cadherin (blue in B) and Six1 (green in C). Merged figures are shown in (D). The position of nuclei was visualized with DAPI, as shown in panel E. Satellite cells were labeled with the co-immunofluorescence of both Pax7 and M-cadherin (arrowheads). A subset of Six1-positive cells was satellite cells (C and D). A subset of Six4-positive cells was also labeled with M-cadherin (thick arrow in F). Arrows indicate myonuclei positive for Six1 or Six4 (C–F). Insets show close-up of satellite cells (labeled by asterisk). (G–N) Immunofluorescence of SM/C-2.6-positive satellite cells in the growth medium (G–J) or in the differentiation medium (K–N) using antibodies to Six1 (G, H, K and L in green) and Six4 (I and M in red). Merged figures are shown in panels J and N. Differential interference contrast (DIC) image showed that the majority of satellite cells were mononuclear fibroblastic cells in the growth medium (G) or formed multinucleated myotubes in the differentiation medium (K). Cultured satellite cells were positive for both Six1 and Six4 (J and N). Scale bars: 20 μm (A–F), 5 μm (insets) and 100 μm (G–N). (O) Nuclear (lane 1) and cytoplasmic (lane 2) extracts from SM/C-2.6-positive satellite cells were analyzed by western blotting with anti-Six5 antibody. For reference, nuclear (lane 3) and cytoplasmic (lane 4) extracts were also prepared from C2C12 cells and analyzed. Arrowheads indicate the positions of the detected Six5 proteins. The position of molecular mass marker is shown on the right.

and used immunofluorescence staining to check for the presence of Six1 and Six4. Six1 immunofluorescence was observed in virtually all muscle satellite cells in the growth medium (Figs. 2G and H). Six4 immunofluorescence was also observed in these satellite cells (Fig. 2I). Although Six1 and Six4 were colocalized in almost all satellite cells, the relative immunofluorescence intensity and subcellular distribution of Six1 and Six4 varied among individual cells (Fig. 2J). To examine whether Six1 and Six4 proteins are present during differentiation, the isolated satellite cells were cultured in the differentiation medium. Most of the satellite cells formed myotubes within 24 hours (Fig. 2K). Myonuclei in the myotubes were positive for Six1 (Figs. 2K and L) and Six4 (Fig. 2M), though the relative immunofluorescence intensities varied among myonuclei (Fig. 2N), as observed in the growth medium (Fig. 2J). We investigated the presence of Six5 in satellite cells by western blotting (Fig. 2O). Nuclear and cytoplasmic extracts from muscle satellite cells cultured in the growth medium were prepared and analyzed by western blotting using anti-Six5 antibody. Six5 protein was detected in nuclear extracts (Fig. 2O lane 1) but not in the cytoplasmic extracts (Fig. 2O lane 2). Furthermore, Six5 protein was detected in nuclear extracts only, but not cytoplasmic extracts, prepared from the control C2C12 mouse myoblast cell (Fig. 2O, lanes 3 and 4, respectively). These results indicate the presence of Six proteins mainly in the nuclei of quiescent, proliferating and differentiating muscle satellite cells.

Overexpression of Six genes inhibits proliferation of muscle satellite cells

Having shown that Six proteins are expressed in quiescent, proliferating and differentiating muscle satellite cells, we next investigated the effects of overexpression of *Six1* as well as *Six4* and *Six5* in isolated muscle satellite cells. In these studies, a retrovirus-mediated system [33] was used to overproduce Six1, Six4 and Six5 proteins. Six proteins and EGFP were connected by IRES. EGFP fluorescence was used to monitor cells transduced with the recombinant retrovirus. Accumulation of Six1, Six4 and Six5 proteins was noted in the nuclei of EGFP-positive cells after infection with a retrovirus harboring *Six1*, *Six4* or *Six5* cDNA, respectively (Supplementary Fig. 1). The nuclear localization was similar to the endogenous Six proteins both *in vivo* and *in vitro* (Figs. 1 and 2).

To analyze the effects of overexpression of *Six* genes on cell proliferation, we assessed the expression of proliferation markers, phospho-histone H3 and Ki67, by immunofluorescence (Fig. 3). Among the cells infected with the control retrovirus, a subset of EGFP-expressing cells was positive for phospho-histone H3 (Fig. 3A, arrowheads). In contrast, the signal of phospho-histone H3 was rarely observed in EGFP-positive cells infected with a retrovirus harboring *Six1*, *Six4* or *Six5* cDNA (Figs. 3B–D). Immunofluorescence of Ki67 was also observed in EGFP-positive cells infected with the control virus (Fig. 3E, arrowheads), but rarely in EGFP-positive cells infected with the retrovirus harboring *Six1*, *Six4* or *Six5* cDNA (Figs. 3F–H). To quantify cell proliferation, we determined the percentage of Ki67-positive cells among the EGFP-positive cells (Fig. 3I). The Ki67 index was $15.1 \pm 2.2\%$ in control, but significantly reduced to $5.7 \pm 1.4\%$, $4.8 \pm 1.9\%$ and $5.4 \pm 1.3\%$ in cells infected with retrovirus harboring *Six1*, *Six4* and *Six5*, respectively, indicating that overproduction of these Six proteins suppresses the proliferation of satellite cells.

Overexpression of Six1 promotes and excess Six4 and Six5 repress differentiation of muscle satellite cells

To investigate the effects of *Six* gene overexpression on the differentiation of muscle satellite cells, these cells were cultures in differentiation medium after retrovirus infection. EGFP signals were detected in myotubes and scattered mononuclear cells in the control experiment (Fig. 4A). Infection of the satellite cells with a retrovirus harboring *Six1* resulted in a considerable increase in the size of EGFP-positive myotubes relative to the control (Fig. 4B). On the other hand, many scattered single cells were positive for EGFP and fewer myotubes were observed when the retrovirus harboring *Six4* or *Six5* was used for infection (Figs. 4C and D). To assess cell differentiation, the fusion index of EGFP-positive cells (see Materials and methods) and the mean number of nuclei in EGFP/skeletal muscle myosin-double positive cells were determined after viral infection (Figs. 4E and F). The fusion index was $63.9 \pm 3.62\%$ in cells infected with the control retrovirus, and significantly higher ($82.3 \pm 2.39\%$) in cells infected with the retrovirus harboring *Six1* (Fig. 4E). In contrast, the index was $15.0 \pm 3.19\%$ and $13.8 \pm 2.72\%$ in Six4- and Six5-overexpressing cells, respectively; the latter values were significantly lower than the control. The mean number of nuclei in myosin-positive cells was 2.30 ± 0.20 when the control virus was used for infection (Fig. 4F), but increased to 3.82 ± 0.39 in cells infected with retrovirus harboring *Six1*, and decreased to 1.18 ± 0.06 and 1.16 ± 0.05 by infection with retrovirus overexpressing *Six4* and *Six5*, respectively. These results indicate that overproduction of Six1 stimulates while that of Six4 or Six5 inhibits the differentiation of muscle satellite cells in the differentiation medium.

To confirm the above effects of *Six* genes overexpression on satellite cell differentiation, the fusion index of EGFP-positive cells and the mean number of nuclei in myosin-positive cells were determined in the growth medium (Fig. 4G and H). The fusion

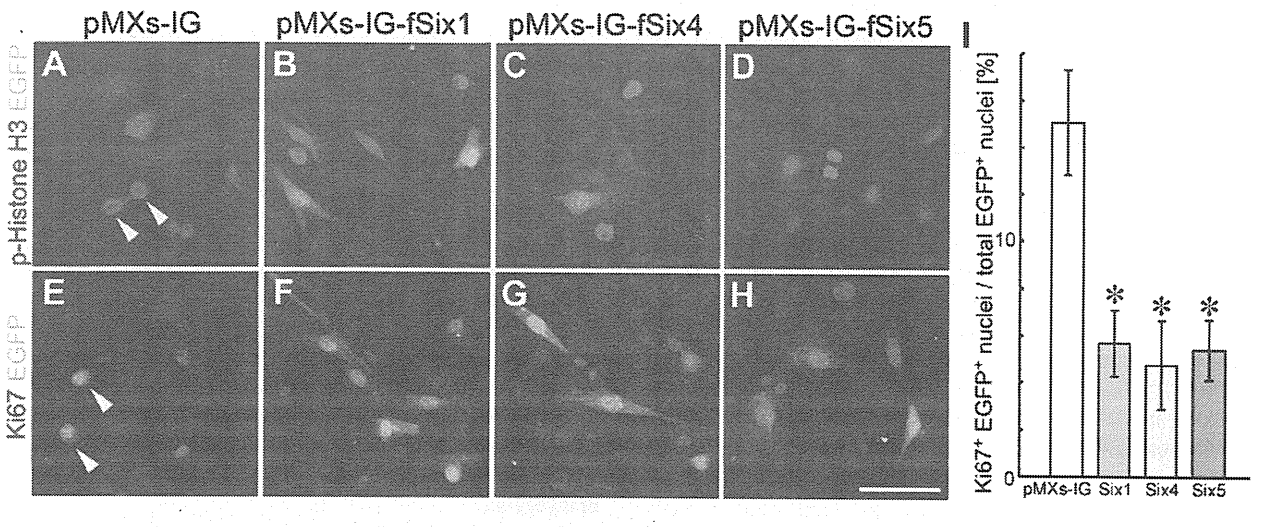

Fig. 3 – Overproduction of Six1, Six4 and Six5 interferes with proliferation of muscle satellite cells. Immunofluorescence of satellite cells infected with control retrovirus (A and E) or retrovirus harboring *Six1* (B and F), *Six4* (C and G) or *Six5* (D and H) in the growth medium using antibodies to phospho-histone H3 (A–D) or Ki67 (E–H), shown in red. Arrowheads point to EGFP-positive cells immunostained with anti-phospho-histone H3 (A) or anti-Ki67 (E) antibodies. Scale bar: 50 μm. (I) The percentages of Ki67-positive nuclei among EGFP-positive cells infected with control retrovirus (pMXs-IG) and retrovirus harboring *Six1* (Six1), *Six4* (Six4) or *Six5* (Six5) were calculated. Data are mean ± SEM of three independent cell isolates. *$p < 0.001$, compared with pMXs-IG.

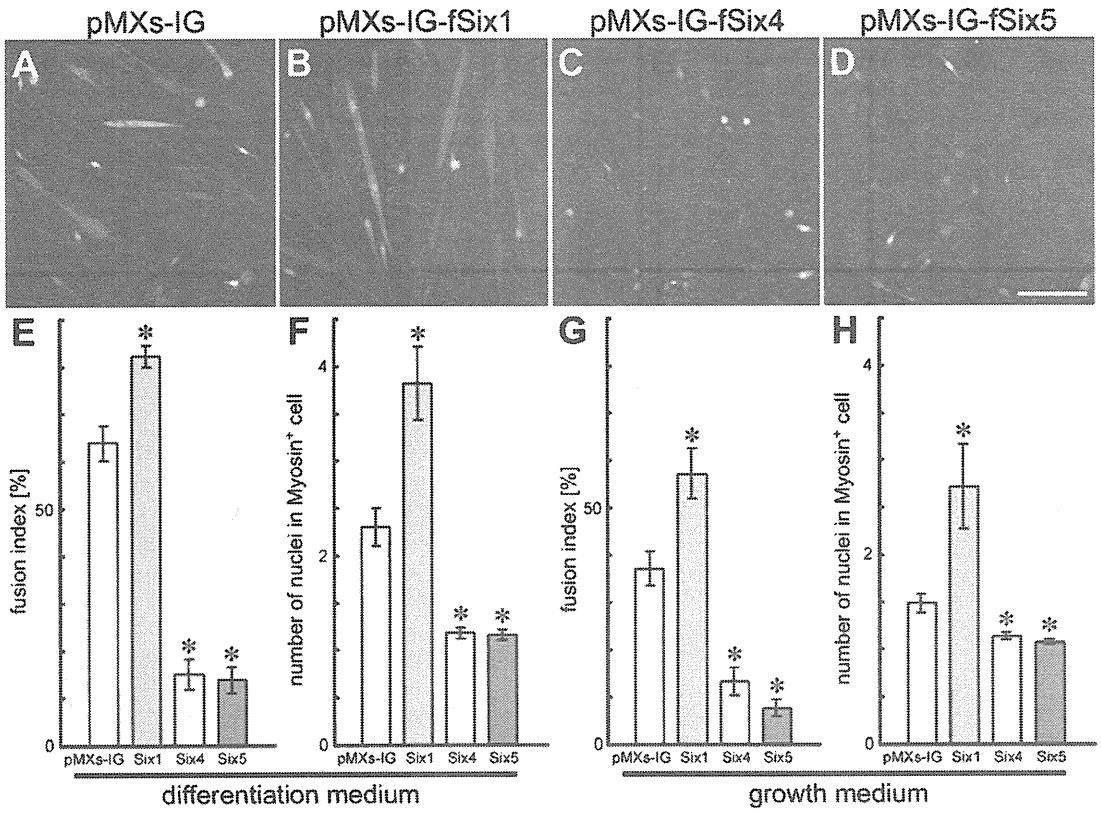

Fig. 4 – Effects of overproduction of Six1, Six4 and Six5 on differentiation of muscle satellite cells. Representative images of EGFP-positive cells infected with control retrovirus (A) and retrovirus harboring *Six1* (B), *Six4* (C) or *Six5* (D) in the differentiation medium. Nuclei were stained with DAPI (blue). Scale bar: 100 μm. The percentage of nuclei within myotubes (fusion index) was calculated among the EGFP-positive cells (E and G) and the number of nuclei in EGFP and skeletal muscle myosin-double positive cells was counted and averaged (F and H) in the differentiation medium or growth medium, respectively, following infection with control retrovirus (pMXs-IG) or retrovirus harboring *Six1* (Six1), *Six4* (Six4) or *Six5* (Six5). Data are mean ± SEM of three independent cell isolates. *$p < 0.001$, compared with pMXs-IG.

index was 37.2 ± 3.73% and the mean number of nuclei in myosin-positive cells was 1.48 ± 0.10 in cells infected with the control retrovirus (Figs. 4G and H, pMXs-IG). These observations clearly indicate that differentiation occurs in a subset of satellite cells even in the growth medium, although the extent of differentiation is lower than that in the differentiation medium. Infection with a retrovirus harboring *Six1* increased the fusion index to 57.3 ± 5.35% as well as the mean number of nuclei in myosin-positive cells to 2.72 ± 0.45. On the other hand, in cells infected with retrovirus harboring *Six4* or *Six5*, the fusion index and mean number of nuclei in myosin-positive cells were reduced to 13.3 ± 2.93% or 7.57 ± 1.77% and 1.14 ± 0.04 or 1.07 ± 0.02, respectively (Figs. 4G and H). These results indicate that even in the growth medium, overproduction of Six1 promotes differentiation, whereas overproduction of Six4 or Six5 represses differentiation of muscle satellite cells.

Overproduction of Six4 or Six5 inhibits differentiation of satellite cells by down-regulation of myogenin expression

To determine the mechanism of Six1-induced enhancement and Six4-/Six5-induced inhibition of differentiation of satellite cells, we investigated the expression of key regulators of muscle differentiation and regeneration (Fig. 5).

Myogenin is expressed in myoblasts and plays an important role in muscle development [34,35] and its expression is positively controlled by *Six* genes [21,26,27]. The percentage of myogenin-positive cells in EGFP-positive satellite cells infected with the control retrovirus was 18.9 ± 1.68% (Figs. 5A, E, arrows and Q). Overexpression of *Six1* significantly increased the number of myogenin-positive cells to 27.5 ± 3.33% of EGFP-positive cells (Figs. 5B, F, arrows and Q). In contrast, the percentages of myogenin-positive cells were significantly reduced to 4.18 ± 1.71% and 2.49 ± 1.11% in satellite cells infected with the retrovirus harboring *Six4* and *Six5*, respectively (Figs. 5C, D, G, H, arrowheads and Q). These data suggest that misexpression of *Six1* promotes the expression of myogenin, whereas overexpression of *Six4* and *Six5* results in down-regulation of myogenin.

To investigate the effects of overproduction of Six proteins on the activation of muscle satellite cells, we analyzed the expression of MyoD and Pax7. Damage or injury of the skeletal muscle activates quiescent satellite cells as evident by coexpression of MyoD and Pax7 [3]. Following the induction of MyoD and Pax7 expression, most satellite cells undergo proliferation. Infection of satellite cells with the

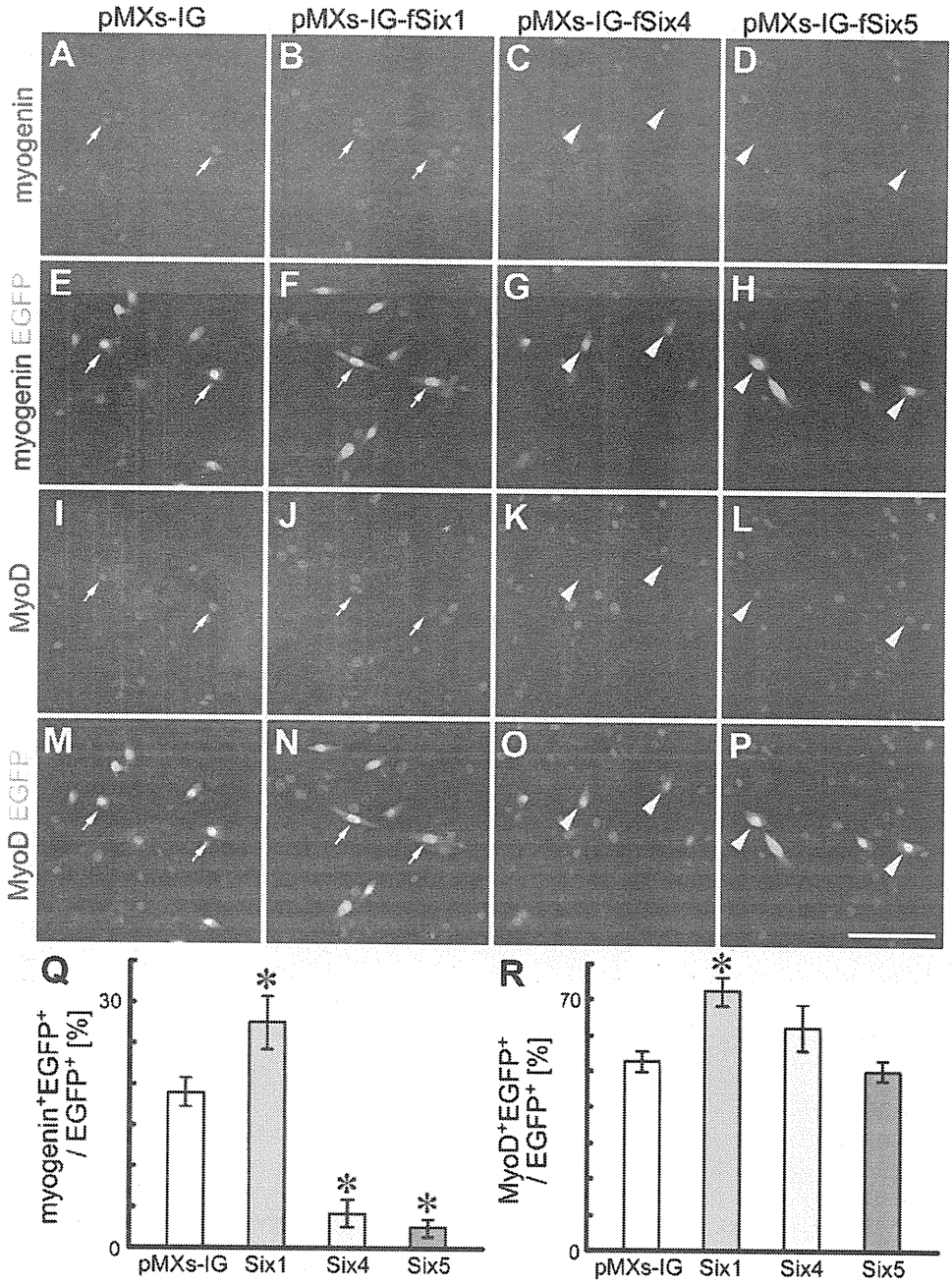

Fig. 5 – Effects of overproduction of Six proteins on the expression of myogenin and MyoD in muscle satellite cells. Immunofluorescence of satellite cells infected with control retrovirus (A, E, I and M) or retrovirus harboring *Six1* (B, F, J and N), *Six4* (C, G, K and O) or *Six5* (D, H, L and P) in growth medium using antibodies to myogenin (A–H in red) and MyoD (I–P in red). Arrows show colocalization of myogenin, MyoD and EGFP. Arrowheads point to weak signals of myogenin immunofluorescence in MyoD and EGFP-positive cells. Scale bar: 100 μm. The percentages of myogenin- and MyoD-positive cells were calculated among the EGFP-positive cells (Q and R). Data are mean ± SEM calculated from three similar results obtained from two independent cell isolates. *$p < 0.05$, compared with pMXs-IG.

control retrovirus resulted in the appearance of MyoD immunofluorescence in the nuclei of 53.9 ± 5.04% of EGFP-positive cells (Figs. 5I, M, arrows and R). The percentages of MyoD-positive cells increased significantly to 72.2 ± 3.95% with retrovirus harboring *Six1* (Figs. 5J, N, arrows and R), but only to 61.8 ± 6.45% and 50.0 ± 2.97% with retroviruses harboring *Six4* and *Six5*, respectively, which were not statistically different from that of the control (Figs. 5K, L, O, P, arrowheads and R). Cultured muscle satellite cells also expressed Pax7 (data not shown). The percentages of Pax7-positive cells were not apparently altered by the infections of retroviruses harboring any of the *Six* genes, compared with the control retrovirus (data not shown). The above results indicate that overexpression of *Six4* and

Six5 results in down-regulation of myogenin, without altering MyoD and Pax7 expression, suggesting that overproduction of Six4 or Six5 negatively regulates the differentiation of satellite cells by repressing the expression of myogenin, while they do not affect the activation of these cells.

Six5 knockdown promotes proliferation of muscle satellite cells

We also examined the functions of *Six* genes using the Stealth small interfering RNA (siRNA)-mediated knockdown approach. The knockdown efficiency of each siRNA against individual *Six* genes, *Six1*, *Six4* and *Six5*, was validated in C2C12 cell line (Supplementary Fig. 2). In muscle satellite cells derived from the extensor digitorum longus (EDL) of 8- to 12-week-old wild-type mice, the endogenous level of Six proteins was not affected by the transfection of negative control siRNA (Fig. 6A, data not shown). The use of Six1 siRNA, Six4 siRNA and Six5 siRNA reduced Six1, Six4 and Six5 protein levels to around 25%, 25% and 40%, respectively, compared to the negative control, when assayed 48 hours after transfection (Fig. 6A).

To investigate the roles of *Six* genes in the proliferation of muscle satellite cells, cell number was counted at 48 hours after transfection of each siRNA and compared to the number of muscle satellite cells transfected with negative control siRNA (Fig. 6B). Six1 siRNA and Six4 siRNA did not significantly change the proportion of such cells (1.33 ± 0.56 and 0.87 ± 0.12-fold, respectively). In contrast, transfection of Six5 siRNA robustly increased the ratio to 5.4 ± 0.71-fold.

To analyze whether knockdown of *Six* genes altered differentiation properties of muscle satellite cells, we performed immunofluorescence of skeletal muscle myosin to assess the extent of muscle differentiation. Twelve hours after transfection of each siRNA, the medium was replaced with the differentiation medium and cells were incubated for additional 36 hours. The proportion of

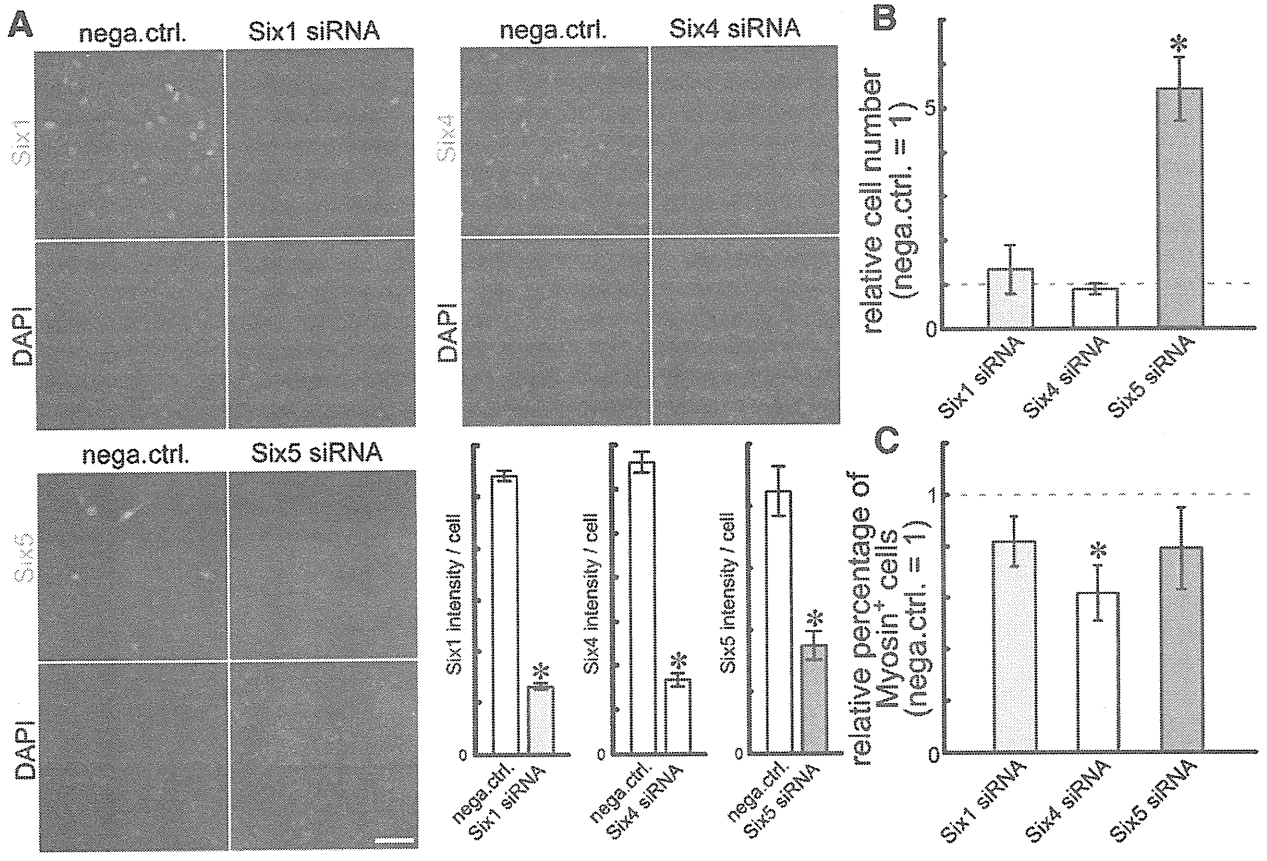

Fig. 6 – Effects of knockdown of *Six1*, *Six4* and *Six5* on proliferation and differentiation of satellite cells. (A) Immunofluorescence of satellite cells transfected with negative control siRNA, Six1 siRNA, Six4 siRNA and Six5 siRNA in growth medium using antibodies to Six1, Six4 and Six5 shown in green. Nuclei were stained with DAPI (blue). The intensity of immunofluorescence of typical result was densitometrically analyzed and displayed in bar graphs. Data are mean ± SEM. *$p < 0.01$, compared with negative control siRNA. Scale bar: 50 μm. Note no obvious increase in picnotic nuclei stained with DAPI in the siRNA-transfected cells, suggesting the marginal cytotoxicity caused by Stealth siRNA. (B) Forty-eight hours after transfection of siRNAs, the cell numbers transfected with Six1 siRNA, Six4 siRNA and Six5 siRNA were counted and normalized by that of negative control siRNA. Data are mean ± SEM of three independent cell isolates. *$p = 0.004$, compared with negative control siRNA. (C) Satellite cells were transfected with siRNAs and cultured in differentiation medium. The percentage of skeletal muscle myosin-positive cells among total cells treated with Six1 siRNA, Six4 siRNA and Six5 siRNA was determined and expressed relative to that of negative control siRNA. Data are mean ± SEM of four independent cell isolates. *$p = 0.01$, compared with the negative control siRNA.

skeletal muscle myosin-positive cells among total cells was determined and normalized by that of muscle satellite cells transfected with negative control siRNA (Fig. 6C). The relative ratios of skeletal muscle myosin-positive cells were reduced to 0.81 ± 0.10, $0.61 \pm 0.11$and 0.79 ± 0.16-fold by the transfection of Six1 siRNA, Six4 siRNA and Six5 siRNA, respectively. However, only the reduction provided by Six4 siRNA was statistically significant. These results indicate that Six5 regulates the proliferation of muscle satellite cells while Six4 plays a role in the differentiation of these cells.

Altered proliferation of muscle satellite cells in Six4$^{+/-}$Six5$^{-/-}$ mice

We further analyzed the roles of *Six* genes in the proliferation and differentiation of muscle satellite cells by characterizing these cells in *Six* gene-deficient mice. Such analysis would corroborate the data obtained from siRNA-mediated knockdown experiments. However, among the knockout mice of *Six* genes, *Six1*$^{-/-}$ mice die immediately after birth [11] and it is impossible to analyze satellite cells derived from adult skeletal muscles. Since *Six4*$^{-/-}$ and *Six5*$^{-/-}$ mice are viable and do not show apparent muscle phenotypes [16,24,36] (and data not shown), we intercrossed *Six4*$^{+/-}$*Six5*$^{+/-}$ mice to obtain adult with the smallest dosage of *Six* genes. All *Six4*$^{-/-}$*Six5*$^{-/-}$ mice were never born and *Six4*$^{-/-}$*Six5*$^{+/-}$ mice were rarely born in less than Mendelian ratio (data not shown). On the other hand, *Six4*$^{+/-}$*Six5*$^{-/-}$ mice were viable and did not show obvious phenotype in adult skeletal muscles (data not shown). Thus, we were able to evaluate the behavior of satellite cells with the smallest dosage of *Six* genes in *Six4*$^{+/-}$*Six5*$^{-/-}$ mice.

SM/C-2.6-positive cells were isolated from limb and back muscles of 8- to 12-week-old *Six4*$^{+/-}$*Six5*$^{-/-}$ mice and their proliferation and differentiation were compared with those of age-matched wild-type mice (Fig. 7). The total number of muscle satellite cells isolated from *Six4*$^{+/-}$*Six5*$^{-/-}$ mice was not significantly different from those of wild-type mice (data not shown). The isolated satellite cells were plated at two different densities, 6.5×10^3 and 1.3×10^4 cells/cm^2 (Fig. 7A plating) and cultured in the growth medium. The cells were harvested and counted every day for 4 days after plating. One day after plating at low density (6.5×10^3 cells/cm^2), the cell density of satellite cells from *Six4*$^{+/-}$*Six5*$^{-/-}$ mice was significantly higher than that from wild-type mice (Fig. 7A day 1, solid circles). From day 1 to day 4, the density of satellite cells from *Six4*$^{+/-}$*Six5*$^{-/-}$ was consistently higher than that from wild-type (Fig. 7A day 1–day 4, solid circles). When the culture contained a higher density of these cells (1.3×10^4 cells/cm^2), the density of satellite cells from *Six4*$^{+/-}$*Six5*$^{-/-}$ was also consistently higher than that from wild-type after plating (Fig. 7A day 1–day 4, solid squares). Although the satellite cells derived from both genotypes reached a proliferation plateau at 3 days after plating, the cell density at the plateau was also higher in the *Six4*$^{+/-}$*Six5*$^{-/-}$ mice than in wild-type mice (Fig. 7A day 3–day 4, solid squares). Considered together, these results suggest that satellite cells from *Six4*$^{+/-}$*Six5*$^{-/-}$ begin proliferation earlier and grow to a higher cell density, compared to wild-type satellite cells. The possibilities that the observed differences were due to the plating efficiency of the cells or recovery from passage were not excluded.

To analyze whether muscle satellite cells from *Six4*$^{+/-}$*Six5*$^{-/-}$ mice have altered differentiation properties, the satellite cells from wild-type and *Six4*$^{+/-}$*Six5*$^{-/-}$ mice were cultured in the differentiation medium at two different densities, 2×10^4 and 4×10^4 cells/cm^2. We performed immunofluorescence of skeletal muscle myosin to estimate the extent of muscle differentiation. At plating

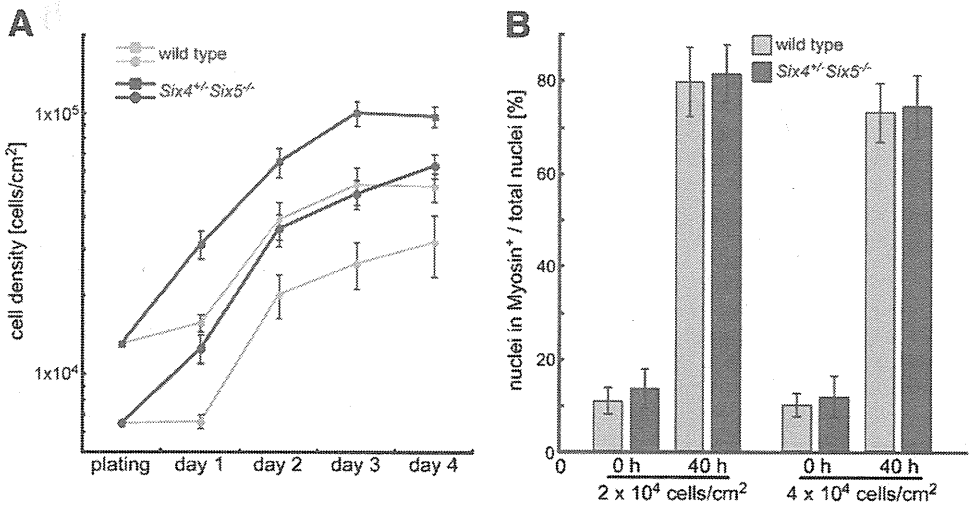

Fig. 7 – Proliferation of muscle satellite cells from *Six4*$^{+/-}$*Six5*$^{-/-}$ and wild-type mice. (A) Isolated satellite cells were plated at two different densities, 6.5×10^3 (circles) and 1.3×10^4 (squares) cells/cm^2. After plating, the cell densities of satellite cells from the wild-type (gray symbols) and *Six4*$^{+/-}$*Six5*$^{-/-}$ (black symbols) mice were calculated at 1 day (day 1), 2 days (day 2), 3 days (day 3) and 4 days (day 4) in the growth medium. Data are mean ± SEM of three independent cell isolates. (B) Satellite cells from wild-type (gray bars) and *Six4*$^{+/-}$*Six5*$^{-/-}$ (black bars) mice were plated at two different densities, 2×10^4 (left side) and 4×10^4 (right side) cells/cm^2. Two hours later, the culture medium was replaced with the differentiation medium to induce differentiation of myotubes. The percentage of nuclei of the satellite cells positive for skeletal muscle myosin immunofluorescence was calculated at medium change to differentiation medium (0 h) and 40 hours after medium change (40 h). Data are mean ± SEM of four independent cell isolates.

(one passage after preparation), the percentage of satellite cells expressing skeletal muscle myosin was not significantly different between wild-type and *Six4*$^{+/-}$*Six5*$^{-/-}$ (data not shown). Two hours after plating, the medium was replaced with the differentiation medium. Satellite cells were collected at 0 and 40 hours after the medium change. At 0 hour, the percentages of skeletal muscle myosin-positive satellite cells were similar in the wild-type (10.7 ± 2.79%) and *Six4*$^{+/-}$*Six5*$^{-/-}$ (13.4 ± 4.29%), when plated at low cell density (2×10^4 cells/cm^2) (Fig. 7B 0 h). At 40 hours after the medium change, the percentage of skeletal muscle myosin-positive cells in wild-type (79.5 ± 7.51%) was similar to that in *Six4*$^{+/-}$*Six5*$^{-/-}$ (81.2 ± 6.30%, Fig. 7B 40 h). Even when satellite cells were plated at high density (4×10^4 cells/cm^2), the percentages of skeletal muscle myosin-positive cells in the wild-type were not significantly different from *Six4*$^{+/-}$*Six5*$^{-/-}$ at 0 and 40 hours (9.91 ± 2.57 and 11.7 ± 4.49% at 0 hour, 73.0 ± 6.34 and 74.3 ± 6.73% at 40 hours, respectively). These results suggest that the differentiation capacity of *Six4*$^{+/-}$*Six5*$^{-/-}$ satellite cells is similar to that of the wild-type. Considered together, the analysis of satellite cells from *Six4*$^{+/-}$*Six5*$^{-/-}$ mice indicates that either *Six4* or *Six5* or both play a role in the regulation of muscle satellite cell proliferation.

Discussion

Muscle satellite cells are one of the most important players in muscle regeneration. Understanding the control mechanisms of their proliferation and differentiation is important for the development of cell-based therapy for muscle disorders such as dystrophy using these cells [37]. The roles of the members of *Six* family genes, especially *Six1*, *Six4* and *Six5*, have been extensively studied during embryonic development of skeletal muscle and the results indicate that they play critical roles in myogenesis [21–23]. However, the involvement of these genes in muscle regeneration and behavior of satellite cells has never been addressed. This study demonstrated, for the first time, the roles of *Six* family genes in muscle satellite cells.

Robust induction of Six1- and Six4-positive cells was observed in regenerating muscle three days after damage by cardiotoxin injection in adult skeletal muscle (Fig. 1). Many of these cells were also positive for MyoD, which is known to be expressed in myoblasts produced rapidly during regeneration, and mitotic marker Ki67. Thus, these cells are considered to be myogenic precursor cells. The quiescent muscle satellite cells marked by Pax7 and M-cadherin in the myofibers were also positive for Six1 and Six4 (Fig. 2). In addition, the muscle satellite cells isolated by SM/C-2.6 antibody are positive for Six1, Six4 and Six5 under proliferation and differentiation conditions (Fig. 2). These observations prompted us to investigate in detail the roles of Six1, Six4 and Six5 in the proliferation and differentiation of muscle satellite cells.

One of the intriguing findings of our study is that *Six* genes were involved in the control of cell proliferation of muscle satellite cells. Overexpression of *Six1*, *Six4* or *Six5* in isolated muscle satellite cells inhibited the proliferation as observed by a reduction in the number of cells positive for phospho-histone H3 and Ki67 (Fig. 3). Conversely, siRNA-mediated knockdown of *Six5* resulted in a robust increase in cell number (Fig. 6). These results mean that the proliferation of muscle satellite cells is negatively regulated when the amount of Six proteins exceeds the normal level, while it is normally repressed by Six5 protein present in the cells. These findings highlight the primary repressive role of Six5 in proliferation of activated satellite cells. Moreover, muscle satellite cells from *Six4*$^{+/-}$*Six5*$^{-/-}$ mice proliferated to higher cell density (Fig. 7), consistent with the role of *Six5* defined in overexpression and knockdown experiments. Because we observed the proliferation of isolated satellite cells, the effect of decreased gene dosage of *Six4* and *Six5* is not through altered niche but is rather cell-autonomous change within the satellite cells. Since inactivation of p16^{INK4a}/cyclinD1/Rb pathway is reported to cause rapid and prolonged mitogenic stimulation [38,39], which is reminiscent of the satellite cells from *Six4*$^{+/-}$*Six5*$^{-/-}$ mice, further analysis of the contribution of Six proteins to the regulatory components of cell cycle is required. Reducing the amount of Six5 protein in muscle satellite cells lead to efficient amplification of the cells without changing the differentiation properties (Fig. 6). This remarkable finding suggests that Six5 may be a good candidate as a molecular target in terms of satellite cell therapy. The amount of Six proteins is maintained at critical level for the normal proliferation of satellite cells. Moreover, variable amount and subcellular localization of each of the Six proteins in individual satellite cells might correlate with their function on proliferation and differentiation (Figs. 1 and 2). These aspects of the Six proteins need to be elucidated in the future.

Six1$^{-/-}$ mice show low cell proliferation capacity in the mouse otic vesicle [11,12]. Overexpression of *Xenopus Optix2*, one of the members of *Xenopus Six* family genes, causes retinal field enlargement due to the augmented proliferation [40]. Six proteins influence the cell cycle by regulating the expression of cyclinA1 [41], c-Myc and cyclinD1 [42,43]. These observations implicate a positive regulatory role for Six proteins in cell proliferation. In sharp contrast, Six proteins repress cell proliferation in muscle satellite cells. This may be related to the function of Six1 in stimulating the differentiation of muscle satellite cells or to cell types that provide different context to Six proteins in terms of their functions.

Another interesting finding is the differential role of Six1 and Six4/Six5 in the control of differentiation of muscle satellite cells. Overproduction of Six1 stimulated muscle differentiation estimated by the fusion index and mean number of nuclei in skeletal muscle myosin-positive cells (Fig. 4). In contrast, overexpression of *Six4* and *Six5* inhibited cell differentiation. The main reason for the differential control of cell differentiation might be related to the differential effects of these Six proteins on the expression of myogenin. In cultured cell transfection assays, Six1, Six2, Six4 and Six5 similarly activated the *myogenin* promoter activity in conjunction with Eya coactivator [26,27]. Similarly, *in vivo*, Six1 and Six4 also activated *myogenin* promoter [26]. In isolated muscle satellite cells, overproduction of Six1 activated the expression of myogenin. In sharp contrast, overproduction of Six4 and Six5 greatly reduced the expression of myogenin (Fig. 5). Thus, Six1 might be the primary Six protein that activates *myogenin* promoter in satellite cells. Indeed, Six1 is known to be required for the proper activation of myogenin in limb muscle development [15]. Moreover, the recent finding of Ski pro-oncogene promotion of C2C12 myoblast differentiation through transcriptional activation of *myogenin* in a complex with Six1 and Eya3 is consistent with this notion [44]. The precise molecular basis for the abovementioned differential effects of Six family proteins on the myogenin

expression is unknown. While it is possible that Six4 and Six5 destabilize the myogenin protein, it is more plausible that the differential effect on myogenin expression is at a transcriptional level. Interestingly, we found a profound reduction in Six1 protein level in the satellite cells upon overexpression of Six4 and Six5 (Supplementary Fig. 3). This suggests the indirect repression mechanisms of myogenin by Six4 and Six5. In this context, the recent report that described the binding of Six1 to the regulatory region of *Six1*, *Six4* and *Six5* [45] supports this notion. Because Six1 shares the binding consensus with Six4 and Six5 [46,47], the possible cross-regulations among *Six* genes has been proposed [45]. On the other hand, Six4 and Six5 may be involved in the direct repression of *myogenin* promoter instead of Six1 that activates the promoter. Considering that Six1 and Six4/Six5 had opposite effects on *myogenin* promoter, it should be noted that Six1 and Six4/Six5 each has a distinct molecular structure. The latter two members have a large C-terminal portion in addition to the conserved Six domain and homeodomain [8,48]. This portion may be involved in the differential function of each Six family protein. If this is the case, it is not surprising that Six1 and Six4/Six5 display differential regulatory role in muscle differentiation.

Because *Six* family genes can modulate the proliferation and differentiation of muscle satellite cells, it is tempting to alter the dosage *Six* genes and analyze their effects on muscle regeneration *in vivo*. We are currently addressing the roles of Six family proteins by examining muscle regeneration in *mdx* mice, in which muscle regeneration occurs more frequently in adults. We are crossing *mdx* mice and defective mice harboring lower gene dosage of *Six* or higher dosage of *Six1*. This approach should uncover the physiological roles of *Six* family genes in the regeneration of skeletal muscles.

Materials and methods

Animals

C57BL/6 mice were purchased from Nihon CLEA (Tokyo, Japan). $Six4^{+/-}$ mice were generated as described previously [16]. $Six5^{+/-}$ mice were generously provided by Dr. S. J. Tapscott [24] and crossed with $Six4^{+/-}$ mice to obtain $Six4^{+/-}Six5^{+/-}$ mice. The intercrosses of $Six4^{+/-}Six5^{+/-}$ mice yielded $Six4^{+/-}Six5^{-/-}$ mice. PCR or Southern blotting was performed to verify the genotypes of offspring as described previously [16,24]. Mice were housed in an environmentally controlled room in the Center for Experimental Medicine of Jichi Medical University, under the guidelines for animal experiments. All experimental protocols were approved by the Ethics Review Committee for Animal Experimentation of Jichi Medical University.

Injection of cardiotoxin

To induce muscle regeneration, cardiotoxin (10 μmol/L 5 μl/body weight (g); Sigma, St. Louis, MO) was injected into the TA muscles of 8- to 12-week-old C57BL/6 mice. Three days after injection, TA muscles were harvested and processed for immunofluorescence.

Immunofluorescence

TA muscles were fixed in 4% paraformaldehyde/phosphate-buffered saline (PBS) for 2 hours at 4 °C. Samples were incubated in 30% sucrose/PBS and then embedded in optimal cutting temperature (OCT) compound (Sakura Finetek, Torrance, CA) for freezing and cryosectioning (10–12 μm in thickness). Cultured cells were fixed with 4% paraformaldehyde/PBS for 10 minutes. The following primary antibodies were used in immunofluorescence: guinea pig anti-Six1 antibody (1:5000 dilution [18]), rat anti-Six1 antibody (1:2000 dilution [10]), guinea pig anti-Six4 antibody (1:2000 dilution, [10]), affinity-purified rabbit anti-Six5 antibody (1:500 dilution, [49]), rabbit anti-laminin antibody (1:1500 dilution, Sigma), rabbit anti-MyoD antibody (1:500 dilution, Santa Cruz Biotechnology, Santa Cruz, CA), mouse anti-Pax7 antibody (hybridoma supernatant, Developmental Studies Hybridoma Bank), rabbit anti-M-cadherin antibody (1:1000 dilution, [50]), mouse anti-skeletal muscle myosin antibody (MY-32) (1:30 dilution, Zymed, San Francisco, CA), rabbit anti-phospho-histone H3 (Ser10) antibody (1:1000 dilution, Millipore, Billerica, MA), rabbit anti-Ki67 antibody (1:30 dilution, YLEM, Italy) and mouse anti-myogenin antibody (F5D) (1:500 dilution, Santa Cruz Biotechnology). For anti-Pax7 antibody, M.O.M. Mouse Ig Blocking Reagent (Vector Laboratories, Burlingame, CA) was used to eliminate the background from endogenous mouse immunoglobulins. To visualize the immunoreactions of primary antibodies, fluorescent-labeled secondary antibodies were used at 1:2000 dilution as follows: anti-rabbit conjugated Cy5 (Amersham Biosciences, Piscataway, NJ), Alexa Fluor 488 anti-rabbit, Alexa Fluor 488 anti-rat, Alexa Fluor 488 anti-guinea pig, Alexa Fluor 546 anti-mouse, Alexa Fluor 546 anti-rabbit, Alexa Fluor 546 anti-rat, Alexa Fluor 546 anti-guinea pig and Alexa Fluor 633 anti-mouse (Molecular Probes/Invitrogen, Carlsbad, CA). 4′6-Diamidino-2-phenylindole (DAPI, Sigma) was used at 50 ng/ml to stain nuclei. The immunofluorescent images were captured with Olympus FV1000 confocal microscope and electronically assigned to red, green or blue channels (Olympus Optical, Tokyo, Japan).

Isolation of satellite cells

Muscle satellite cells were isolated from limb and back muscles of 8- to 12-week-old C57BL/6 or $Six4^{+/-}Six5^{-/-}$ mice by using SM/C-2.6 monoclonal antibody as described previously [4,5]. The sorted cells were expanded on Matrigel (BD, Franklin Lakes, NJ)-coated dishes in a growth medium, DMEM, containing 20% fetal bovine serum, human recombinant bFGF (2.5 ng/ml) (Invitrogen), recombinant mouse HGF (25 ng/ml) (R&D Systems) and heparin (5 μg/ml) (Sigma). To induce differentiation of the satellite cells, the growth medium was replaced with differentiation medium (2% horse serum/DMEM). The culture medium was replaced with a fresh medium every day. Satellite cells derived from EDL were prepared and cultured as described previously [51] and used for siRNA experiments.

Retrovirus vectors and infection

Flag-tagged mouse *Six1*, *Six4* and *Six5* cDNAs [27,52] were cloned into the multiple cloning site upstream of IRES-EGFP of pMXs-IG vector, which was kindly provided by Dr. T. Kitamura [33]. Retroviral particles were produced by transfection of vector plasmids into PLAT-E packaging cells as described previously [33,53]. Muscle satellite cells were plated at 1.3×10^4 cells/cm^2 in growth medium one passage after the preparation. The next day, the medium was replaced with growth medium containing retroviral particles. Two days after infection, the culture medium

was replaced with growth medium or differentiation medium and the cells were incubated for 24 hours for the assays under proliferating condition or differentiation condition, respectively.

Western blotting

Nuclear and cytoplasmic extracts of proliferating muscle satellite cells isolated from 8-week-old *Six4*$^{-/-}$ mice and C2C12 cells were prepared and analyzed by western blotting using anti-Six5 antibody [49] as described previously [27,54].

Fusion index and statistics

Fusion index was calculated as [(number of nuclei in EGFP-positive myotubes (>2 myonuclei) / total nuclei within EGFP-positive cells) × 100%] [55–57]. Differences from the control experiments were tested statistically by the Student's *t*-test. All values are expressed as mean ± SEM. A probability of less than 5% was considered statistically significant.

RNA interference

The Stealth RNAi siRNA Negative Control Med GC Duplex and Stealth Select siRNAs targeted to mouse *Six1*, *Six4* and *Six5* were purchased from Invitrogen (Carlsbad, CA). Six1 siRNA is a mixture of equimolar amounts of Six1-MSS237917, Six1-MSS237918 and Six1-MSS237919. Six4 siRNA consists of Six4-MSS209042, Six4-MSS209043 and Six4-MSS209044. Six5 siRNA consists of Six5-MSS277077, Six5-MSS277078 and Six5-MSS277079. Sequences for each siRNA species were provided by the company under license. The transfection of Stealth siRNA into satellite cells isolated from EDL was performed using Lipofectamine RNAiMAX (Invitrogen) as described previously [51] with slight modifications.

Supplementary materials related to this article can be found online at doi:10.1016/j.yexcr.2010.08.001.

Acknowledgments

We thank Stephen J. Tapscott for *Six5*$^{-/-}$ mice and reading the manuscript and Toshio Kitamura for pMXs-IG plasmid and PLAT-E cell. We are grateful to So-ichiro Fukada for providing SM/C-2.6 antibody and for the helpful discussion. We also thank Hiroko Ikeda, Yuki Takano, Kanako Mogi, Yuko Suto and Miho Akima for the excellent technical assistance. This work was supported by Research Grant No. 17A-10 for Nervous and Mental Disorders from the Ministry of Health, Labour and Welfare, Intramural Research Grant No. 20B-13 for Neurological and Psychiatric Disorders of NCNP, Support Program for Scientific Research Platform in Private Universities (SPSRP) to JMU and a grant from The Nakatomi Foundation.

REFERENCES

[1] A. Mauro, Satellite cell of skeletal muscle fibers, J. Biophys. Biochem. Cytol. 9 (1961) 493–495.
[2] A. Otto, H. Collins-Hooper, K. Patel, The origin, molecular regulation and therapeutic potential of myogenic stem cell populations, J. Anat. 215 (2009) 477–497.
[3] P.S. Zammit, J.P. Golding, Y. Nagata, V. Hudon, T.A. Partridge, J.R. Beauchamp, Muscle satellite cells adopt divergent fates: a mechanism for self-renewal? J. Cell Biol. 166 (2004) 347–357.
[4] S. Fukada, S. Higuchi, M. Segawa, K. Koda, Y. Yamamoto, K. Tsujikawa, Y. Kohama, A. Uezumi, M. Imamura, Y. Miyagoe-Suzuki, S. Takeda, H. Yamamoto, Purification and cell-surface marker characterization of quiescent satellite cells from murine skeletal muscle by a novel monoclonal antibody, Exp. Cell Res. 296 (2004) 245–255.
[5] S. Fukada, A. Uezumi, M. Ikemoto, S. Masuda, M. Segawa, N. Tanimura, H. Yamamoto, Y. Miyagoe-Suzuki, S. Takeda, Molecular signature of quiescent satellite cells in adult skeletal muscle, Stem Cells 25 (2007) 2448–2459.
[6] M.A. Serikaku, J.E. O'Tousa, sine oculis is a homeobox gene required for Drosophila visual system development, Genetics 138 (1994) 1137–1150.
[7] B.N. Cheyette, P.J. Green, K. Martin, H. Garren, V. Hartenstein, S.L. Zipursky, The Drosophila sine oculis locus encodes a homeodomain-containing protein required for the development of the entire visual system, Neuron 12 (1994) 977–996.
[8] K. Kawakami, S. Sato, H. Ozaki, K. Ikeda, Six family genes—structure and function as transcription factors and their roles in development, Bioessays 22 (2000) 616–626.
[9] H. Kobayashi, K. Kawakami, M. Asashima, R. Nishinakamura, Six1 and Six4 are essential for Gdnf expression in the metanephric mesenchyme and ureteric bud formation, while Six1 deficiency alone causes mesonephric-tubule defects, Mech. Dev. 124 (2007) 290–303.
[10] Y. Konishi, K. Ikeda, Y. Iwakura, K. Kawakami, Six1 and Six4 promote survival of sensory neurons during early trigeminal gangliogenesis, Brain Res. 1116 (2006) 93–102.
[11] H. Ozaki, K. Nakamura, J. Funahashi, K. Ikeda, G. Yamada, H. Tokano, H.O. Okamura, K. Kitamura, S. Muto, H. Kotaki, K. Sudo, R. Horai, Y. Iwakura, K. Kawakami, Six1 controls patterning of the mouse otic vesicle, Development 131 (2004) 551–562.
[12] W. Zheng, L. Huang, Z.B. Wei, D. Silvius, B. Tang, P.X. Xu, The role of Six1 in mammalian auditory system development, Development 130 (2003) 3989–4000.
[13] P.X. Xu, W. Zheng, L. Huang, P. Maire, C. Laclef, D. Silvius, Six1 is required for the early organogenesis of mammalian kidney, Development 130 (2003) 3085–3094.
[14] C. Laclef, E. Souil, J. Demignon, P. Maire, Thymus, kidney and craniofacial abnormalities in Six 1 deficient mice, Mech. Dev. 120 (2003) 669–679.
[15] C. Laclef, G. Hamard, J. Demignon, E. Souil, C. Houbron, P. Maire, Altered myogenesis in Six1-deficient mice, Development 130 (2003) 2239–2252.
[16] H. Ozaki, Y. Watanabe, K. Takahashi, K. Kitamura, A. Tanaka, K. Urase, T. Momoi, K. Sudo, J. Sakagami, M. Asano, Y. Iwakura, K. Kawakami, Six4, a putative myogenin gene regulator, is not essential for mouse embryonal development, Mol. Cell. Biol. 21 (2001) 3343–3350.
[17] G. Oliver, R. Wehr, N.A. Jenkins, N.G. Copeland, B.N. Cheyette, V. Hartenstein, S.L. Zipursky, P. Gruss, Homeobox genes and connective tissue patterning, Development 121 (1995) 693–705.
[18] K. Ikeda, S. Ookawara, S. Sato, Z. Ando, R. Kageyama, K. Kawakami, Six1 is essential for early neurogenesis in the development of olfactory epithelium, Dev. Biol. 311 (2007) 53–68.
[19] Y. Suzuki, K. Ikeda, K. Kawakami, Regulatory role of Six1 in the development of taste papillae, Cell Tissue Res. 339 (2010) 513–525.
[20] K. Ikeda, R. Kageyama, Y. Suzuki, K. Kawakami, Six1 is indispensable for production of functional apical and basal progenitors during olfactory epithelial development, Int. J. Dev. Biol. (in press), doi:10.1387/ijdb.093041ki.
[21] R. Grifone, J. Demignon, C. Houbron, E. Souil, C. Niro, M.J. Seller, G. Hamard, P. Maire, Six1 and Six4 homeoproteins are required for Pax3 and Mrf expression during myogenesis in the mouse embryo, Development 132 (2005) 2235–2249.

[22] R. Grifone, C. Laclef, F. Spitz, S. Lopez, J. Demignon, J.E. Guidotti, K. Kawakami, P.X. Xu, R. Kelly, B.J. Petrof, D. Daegelen, J.P. Concordet, P. Maire, Six1 and Eya1 expression can reprogram adult muscle from the slow-twitch phenotype into the fast-twitch phenotype, Mol. Cell. Biol. 24 (2004) 6253–6267.
[23] C. Niro, J. Demignon, S. Vincent, Y. Liu, J. Giordani, N. Sgarioto, M. Favier, I. Guillet-Deniau, A. Blais, P. Maire, Six1 and Six4 gene expression is necessary to activate the fast-type muscle gene program in the mouse primary myotome, Dev. Biol. 338 (2010) 168–182.
[24] T.R. Klesert, D.H. Cho, J.I. Clark, J. Maylie, J. Adelman, L. Snider, E.C. Yuen, P. Soriano, S.J. Tapscott, Mice deficient in Six5 develop cataracts: implications for myotonic dystrophy, Nat. Genet. 25 (2000) 105–109.
[25] S.K. Heath, S. Carne, C. Hoyle, K.J. Johnson, D.J. Wells, Characterisation of expression of mDMAHP, a homeodomain-encoding gene at the murine DM locus, Hum. Mol. Genet. 6 (1997) 651–657.
[26] F. Spitz, J. Demignon, A. Porteu, A. Kahn, J.P. Concordet, D. Daegelen, P. Maire, Expression of myogenin during embryogenesis is controlled by Six/sine oculis homeoproteins through a conserved MEF3 binding site, Proc. Natl. Acad. Sci. U. S. A. 95 (1998) 14220–14225.
[27] H. Ohto, S. Kamada, K. Tago, S.I. Tominaga, H. Ozaki, S. Sato, K. Kawakami, Cooperation of six and eya in activation of their target genes through nuclear translocation of Eya, Mol. Cell. Biol. 19 (1999) 6815–6824.
[28] E.N. Olson, W.H. Klein, bHLH factors in muscle development: dead lines and commitments, what to leave in and what to leave out, Genes Dev. 8 (1994) 1–8.
[29] K. Yun, B. Wold, Skeletal muscle determination and differentiation: story of a core regulatory network and its context, Curr. Opin. Cell Biol. 8 (1996) 877–889.
[30] D.D. Cornelison, B.J. Wold, Single-cell analysis of regulatory gene expression in quiescent and activated mouse skeletal muscle satellite cells, Dev. Biol. 191 (1997) 270–283.
[31] P. Seale, L.A. Sabourin, A. Girgis-Gabardo, A. Mansouri, P. Gruss, M.A. Rudnicki, Pax7 is required for the specification of myogenic satellite cells, Cell 102 (2000) 777–786.
[32] A. Irintchev, M. Zeschnigk, A. Starzinski-Powitz, A. Wernig, Expression pattern of M-cadherin in normal, denervated, and regenerating mouse muscles, Dev. Dyn. 199 (1994) 326–337.
[33] T. Kitamura, Y. Koshino, F. Shibata, T. Oki, H. Nakajima, T. Nosaka, H. Kumagai, Retrovirus-mediated gene transfer and expression cloning: powerful tools in functional genomics, Exp. Hematol. 31 (2003) 1007–1014.
[34] Y. Nabeshima, K. Hanaoka, M. Hayasaka, E. Esumi, S. Li, I. Nonaka, Myogenin gene disruption results in perinatal lethality because of severe muscle defect, Nature 364 (1993) 532–535.
[35] P. Hasty, A. Bradley, J.H. Morris, D.G. Edmondson, J.M. Venuti, E.N. Olson, W.H. Klein, Muscle deficiency and neonatal death in mice with a targeted mutation in the myogenin gene, Nature 364 (1993) 501–506.
[36] P.S. Sarkar, B. Appukuttan, J. Han, Y. Ito, C. Ai, W. Tsai, Y. Chai, J.T. Stout, S. Reddy, Heterozygous loss of Six5 in mice is sufficient to cause ocular cataracts, Nat. Genet. 25 (2000) 110–114.
[37] M.A. Rudnicki, F. Le Grand, I. McKinnell, S. Kuang, The molecular regulation of muscle stem cell function, Cold Spring Harb. Symp. Quant. Biol. 73 (2008) 323–331.
[38] M. Serrano, H. Lee, L. Chin, C. Cordon-Cardo, D. Beach, R.A. DePinho, Role of the INK4a locus in tumor suppression and cell mortality, Cell 85 (1996) 27–37.
[39] J.L. Dean, A.K. McClendon, K.R. Stengel, E.S. Knudsen, Modeling the effect of the RB tumor suppressor on disease progression: dependence on oncogene network and cellular context, Oncogene 29 (2010) 68–80.
[40] M.E. Zuber, M. Perron, A. Philpott, A. Bang, W.A. Harris, Giant eyes in Xenopus laevis by overexpression of XOptx2, Cell 98 (1999) 341–352.
[41] R.D. Coletta, K. Christensen, K.J. Reichenberger, J. Lamb, D. Micomonaco, L. Huang, D.M. Wolf, C. Muller-Tidow, T.R. Golub, K. Kawakami, H.L. Ford, The Six1 homeoprotein stimulates tumorigenesis by reactivation of cyclin A1, Proc. Natl. Acad. Sci. U. S. A. 101 (2004) 6478–6483.
[42] Y. Yu, E. Davicioni, T.J. Triche, G. Merlino, The homeoprotein six1 transcriptionally activates multiple protumorigenic genes but requires ezrin to promote metastasis, Cancer Res. 66 (2006) 1982–1989.
[43] X. Li, K.A. Oghi, J. Zhang, A. Krones, K.T. Bush, C.K. Glass, S.K. Nigam, A.K. Aggarwal, R. Maas, D.W. Rose, M.G. Rosenfeld, Eya protein phosphatase activity regulates Six1-Dach-Eya transcriptional effects in mammalian organogenesis, Nature 426 (2003) 247–254.
[44] H. Zhang, E. Stavnezer, Ski regulates muscle terminal differentiation by transcriptional activation of Myog in a complex with Six1 and Eya3, J. Biol. Chem. 284 (2009) 2867–2879.
[45] Y. Liu, A. Chu, I. Chakroun, U. Islam, A. Blais, Cooperation between myogenic regulatory factors and SIX family transcription factors is important for myoblast differentiation, Nucleic Acids Res. (in press), doi:10.1093/nar/gkq585.
[46] Z. Ando, S. Sato, K. Ikeda, K. Kawakami, Slc12a2 is a direct target of two closely related homeobox proteins, Six1 and Six4, FEBS J. 272 (2005) 3026–3041.
[47] S. Sato, M. Nakamura, D.H. Cho, S.J. Tapscott, H. Ozaki, K. Kawakami, Identification of transcriptional targets for Six5: implication for the pathogenesis of myotonic dystrophy type 1, Hum. Mol. Genet. 11 (2002) 1045–1058.
[48] K. Kawakami, H. Ohto, K. Ikeda, R.G. Roeder, Structure, function and expression of a murine homeobox protein AREC3, a homologue of Drosophila sine oculis gene product, and implication in development, Nucleic Acids Res. 24 (1996) 303–310.
[49] H. Ohto, T. Takizawa, T. Saito, M. Kobayashi, K. Ikeda, K. Kawakami, Tissue and developmental distribution of Six family gene products, Int. J. Dev. Biol. 42 (1998) 141–148.
[50] K. Ojima, A. Uezumi, H. Miyoshi, S. Masuda, Y. Morita, A. Fukase, A. Hattori, H. Nakauchi, Y. Miyagoe-Suzuki, S. Takeda, Mac-1(low) early myeloid cells in the bone marrow-derived SP fraction migrate into injured skeletal muscle and participate in muscle regeneration, Biochem. Biophys. Res. Commun. 321 (2004) 1050–1061.
[51] Y. Ono, V.F. Gnocchi, P.S. Zammit, R. Nagatomi, Presenilin-1 acts via Id1 to regulate the function of muscle satellite cells in a gamma-secretase-independent manner, J. Cell Sci. 122 (2009) 4427–4438.
[52] H. Ozaki, Y. Watanabe, K. Ikeda, K. Kawakami, Impaired interactions between mouse Eya1 harboring mutations found in patients with branchio-oto-renal syndrome and Six, Dach, and G proteins, J. Hum. Genet. 47 (2002) 107–116.
[53] S. Morita, T. Kojima, T. Kitamura, Plat-E: an efficient and stable system for transient packaging of retroviruses, Gene Ther. 7 (2000) 1063–1066.
[54] K. Kawakami, K. Yanagisawa, Y. Watanabe, S. Tominaga, K. Nagano, Different factors bind to the regulatory region of the Na+, K(+)-ATPase alpha 1-subunit gene during the cell cycle, FEBS Lett. 335 (1993) 251–254.
[55] V. Jacquemin, D. Furling, A. Bigot, G.S. Butler-Browne, V. Mouly, IGF-1 induces human myotube hypertrophy by increasing cell recruitment, Exp. Cell Res. 299 (2004) 148–158.
[56] V. Horsley, K.M. Jansen, S.T. Mills, G.K. Pavlath, IL-4 acts as a myoblast recruitment factor during mammalian muscle growth, Cell 113 (2003) 483–494.
[57] V. Horsley, B.B. Friday, S. Matteson, K.M. Kegley, J. Gephart, G.K. Pavlath, Regulation of the growth of multinucleated muscle cells by an NFATC2-dependent pathway, J. Cell Biol. 153 (2001) 329–338.

The American Journal of Pathology, Vol. 176, No. 5, May 2010

DOI: 10.2353/ajpath.2010.090887

Musculoskeletal Pathology

Genetic Background Affects Properties of Satellite Cells and *mdx* Phenotypes

So-ichiro Fukada,* Daisuke Morikawa,* Yukiko Yamamoto,* Tokuyuki Yoshida,* Noriaki Sumie,* Masahiko Yamaguchi,* Takahito Ito,* Yuko Miyagoe-Suzuki,† Shin'ichi Takeda,† Kazutake Tsujikawa,* and Hiroshi Yamamoto*

From the Department of Immunology, Graduate School of Pharmaceutical Sciences, Osaka University, Osaka; and the Department of Molecular Therapy,† National Institute of Neuroscience, National Center of Neurology and Psychiatry, Tokyo, Japan*

Duchenne muscular dystrophy (DMD) is the most common lethal genetic disorder of children. The *mdx* (C57BL/10 background, C57BL/10-*mdx*) mouse is a widely used model of DMD, but the histopathological hallmarks of DMD, such as the smaller number of myofibers, accumulation of fat and fibrosis, and insufficient regeneration of myofibers, are not observed in adult C57BL/10-*mdx* except for in the diaphragm. In this study, we showed that DBA/2 mice exhibited decreased muscle weight, as well as lower myofiber numbers after repeated degeneration–regeneration cycles. Furthermore, the self-renewal efficiency of satellite cells of DBA/2 is lower than that of C57BL/6. Therefore, we produced a DBA/2-*mdx* strain by crossing DBA/2 and C57BL/10-*mdx*. The hind limb muscles of DBA/2-*mdx* mice exhibited lower muscle weight, fewer myofibers, and increased fat and fibrosis, in comparison with C57BL/10-*mdx*. Moreover, remarkable muscle weakness was observed in DBA/2-*mdx*. These results indicate that the DBA/2-*mdx* mouse is a more suitable model for DMD studies, and the efficient satellite cell self-renewal ability of C57BL/10-*mdx* might explain the difference in pathologies between humans and mice. *(Am J Pathol 2010, 176:2414–2424; DOI: 10.2353/ajpath.2010.090887)*

Duchenne muscular dystrophy (DMD) is a progressive and lethal X-linked muscular disorder caused by mutations in the dystrophin gene.[1] The dystrophin gene encodes a 427-kDa cytoskeletal protein that forms the dystrophin/glycoprotein complex at the sarcolemma with α- and β-dystroglycans, α-, β-, γ-, and δ-sarcoglycans, and other molecules, and links the cytoskeleton of myofibers to the extracellular matrix in skeletal muscle.[2,3] The lack of dystrophin in the sarcolemma disturbs the assembly of the dystrophin/glycoprotein complex and causes instability of the muscle membrane, leading to muscle degeneration and myofiber loss. The histopathological hallmarks of DMD include degeneration, necrosis, accumulation of fat and fibrosis, and insufficient regeneration of myofibers accompanied by a loss of myofibers.[4] Therefore, the manifestations of DMD are considered to result from an imbalance between degeneration and regeneration.

The function and structure of dystrophin has been elucidated by studies of a variety of dystrophin-deficient animals. Among these animal models, the *mdx* mouse (the correct nomenclature is C57BL/10-*Dmd*^{mdx}), first described in1984, is the most prolific. A spontaneous mutation (*mdx*) arose in an inbred colony of C57BL/10 mice, which have a high level of serum pyruvate kinase.[5] The muscle pathology of the mice includes active fiber necrosis, cellular infiltration, a wide range of fiber sizes, and numerous centrally nucleated regenerating fibers. However, in contrast to DMD, replacement of muscle with fat and fibrosis is not prominent, and no losses of muscle fiber and muscle weight are observed in the skeletal muscle of *mdx* mice except in the diaphragm.[6,7] In contrast, most of the limb muscles of the *mdx* mouse maintain hypertrophy and increased skeletal muscle mass throughout much of their life span.[8] One reason for the difference between DMD and *mdx* is explained by the up-regulation of expression of utrophin, a homolog of dystrophin.[9,10] Another reason has been supposed to be the excellent regeneration capacity of *mdx* com-

Supported by grants-in-aid from the Japanese Ministries of Health, Labor and Welfare, and Education, Culture, Sports, Science and Technology, Sports and Culture of Japan, and the Suzuken Memorial Foundation.

S.F. and D.M. contributed equally to this work.

Accepted for publication December 22, 2009.

Address reprint requests to So-ichiro Fukada, Ph.D., Department of Immunology, Graduate School of Pharmaceutical Sciences, Osaka University, 1-6 Yamada-oka, Suita, Osaka 565-0871, Japan. E-mail: fukada@phs.osaka-u.ac.jp.

pared with DMD. However, this hypothesis has not been verified.

Regeneration of skeletal muscle depends on the competence of muscle satellite cells. Muscle satellite cells, which account for 2 to 5% of the total nuclei in adult skeletal muscle, play a major role in muscle regeneration.[11] Under normal conditions, satellite cells are found external to the myofiber plasma membrane and beneath the muscle basal lamina,[12] and they are mitotically quiescent in adult skeletal muscle.[13] When activated by muscle damage, satellite cells proliferate, differentiate, fuse with each other or injured myofibers, and eventually regenerate mature myofibers. During the regenerative processes, satellite cells not only produce large amounts of muscle, but also renew themselves to maintain their own population.[14] In fact, it is reported that the satellite cell pool of C57BL/10 continues to respond efficiently even when the skeletal muscle is subjected to as many as 50 cycles of severe damage.[15] Therefore, it is thought that maintenance of the satellite cell pool is indispensable to retain the long-term regenerative potential for skeletal muscle injury, including in muscular dystrophies.

To investigate genetic differences in long-term regeneration potential, we first induced repeated degeneration–regeneration cycles in four inbred strains of mice. Among these strains, C57BL/6, a widely used strain akin to C57BL/10, was tolerant of repeated injury. This is consistent with the results of C57BL/10 previously described.[15] In contrast, among four inbred strains, DBA/2 mice exhibited the most remarkable skeletal muscle loss and impaired regeneration after repeated injury. Importantly, the self-renewal potential of DBA/2 satellite cells was significantly lower than that of C57BL/6. In addition, *in vitro* colony formation and proliferation assays indicated that intrinsic difference between C57BL/6 and DBA/2 satellite cells exist. Finally, we crossed the *mdx* genotype with the DBA/2 for more than five generations. At the fifth backcross, the mice are not yet fully congenic (D2.B10-*DMD*^{mdx}), and thus we refer to them as DBA/2-*mdx* hereafter. We investigated their phenotypes. Intriguingly, severe loss of skeletal muscle weight, decreased myofiber number, increased fat and fibrosis volume, and apparent muscle weakness were observed in the DBA/2-*mdx* mice. These results indicate that the intrinsic genetic program affects the properties of satellite cells, and DBA/2-*mdx* will be a more useful model of DMD than C57BL/10-*mdx*. It is also speculated that the high self-renewal potential of C57BL/10 satellite cells might explain the difference in pathologies between humans and mice.

Materials and Methods

Mice

Six-week-old, specific pathogen-free, BALB/c, C3H/HeN, C57BL/6, and DBA/2 mice were purchased from Charles River Japan (Yokohama, Japan). Six-week-old, specific pathogen-free C57BL/10 mice were purchased from Shimizu Laboratory Supplies Co., Ltd (Kyoto, Japan). Specific pathogen-free *mdx* mice (of C57BL/10 background) were provided by Central Laboratories of Experimental Animals (Kanagawa, Japan) and maintained in our animal facility by brother-sister matings. *Mdx* of C57BL/10 background were backcrossed into DBA/2 genetic background. Mice backcrossed more than five generations were used in this study. Genotyping was performed according to previous reports.[16] All procedures for experimental animals were approved by the Experimental Animal Care and Use Committee at Osaka University.

Muscle Injury

Muscle injury was induced by injecting cardiotoxin (10 μmol/L in saline, Wako Pure Chemical Industries, Tokyo, Japan) into tibialis anterior (50 μl), gastrocnemius (150 μl), and quadriceps femoris (100 μl) muscles as described.[17] All injections were first done when mice were 8 to 10 weeks of age.

Histological Analysis

Tibialis anterior, gastrocnemius, and quadriceps femoris muscles were isolated and frozen in liquid nitrogen-cooled isopentane (Wako Pure Chemical Industries). Cryosections (10 μm) were stained with H&E, Oil red-O (Sigma-Aldrich, St. Louis, MO), or Sirius Red (Sigma-Aldrich).

Immunohistochemistry

For immunohistochemical examinations, transverse cryosections (6 μm) were stained with various antibodies. Monoclonal rat anti-laminin α2 (1:200; clone: 4H8-2) and mouse anti-Pax7 antibodies were purchased from Alexis Biochemical (Lausen, Switzerland) and Developmental Studies Hybridoma Bank (Iowa, IA), respectively. For Pax7 staining, a M.O.M. kit (Vector Laboratories, Burlingame, CA) was used to block endogenous mouse IgG. After the first staining at 4°C overnight, sections were reacted with secondary antibodies conjugated with Alexa 488 or Alexa 568 (Molecular Probes, Eugene, OR). Sections were shielded using Vectashield (Vector Laboratories, Inc). The signals were recorded photographically using an Axiophot microscope (Carl Zeiss, Oberkochen, Germany).

Preparation of Muscle Satellite Cells and Culture

Satellite cells were isolated from uninjured adult skeletal muscle using biotinylated-SM/C-2.6[18] and IMag methods (BD Immunocytometry Systems, Mountain View, CA) as described in a previous report.[17] Satellite cells were cultured in a growth medium of high-glucose Dulbecco's modified Eagle's medium (Sigma-Aldrich) containing 20% fetal calf serum (Trace Biosciences, N.S.W., Australia), 2.5 ng/ml basic fibroblast growth factor (PeproTech, London, UK), leukemia inhibitory factor (Alexis Biochemical), and penicillin (100 U/ml)-streptomycin

(100 μg/ml) (Gibco BRL, Gaithersburg, MD) on culture dishes coated with Matrigel (BD Bioscience, San Diego, CA).

Colony Forming Assay

Clonal cultures of freshly isolated satellite cells were performed in 96-well plates coated with type I collagen (Sumilon, Tokyo, Japan) in growth medium for a week. The frequency of colony formation and number of cells in each well were counted under a phase-contrast microscope.

Cell Proliferation Assay

Isolated satellite cells were cultured in growth medium for 3 to 4 days, and expanded primary myoblasts were harvested and additional culture was performed in 96-well dishes for 1 day. Eight hours later, bromodeoxyuridine (BrdU) uptake was quantified using the Cell Proliferation ELISA, BrdU Kit (Roche Diagnostics, Basel, Switzerland) and a microplate reader (Model 680, Bio-Rad, Hercules, CA).

Measurement of Sizes of Myofibers and Oil Red-O-Positive and Fibrotic Areas

Image J software was used to measure myofiber sizes and Oil red-O- and Sirius Red-positive areas.

Evans Blue Dye Injection

Evans blue (Wako Pure Chemical Industries) was dissolved in PBS and injected intraperitoneally into mice (1 mg/100 μl/10g body weight).[19] Sixteen to 18 hours later, muscle tissues were removed, and frozen in liquid nitrogen-cooled isopentane. The muscle fibers with Evans Blue incorporated were then counted as injured muscles.

Muscle Endurance and Grip Strength Test

The muscle endurance test was referred to the studies by Handschin et al.[20] In brief, we used a MK-680S treadmill (Muromachi Kikai Co., Ltd., Tokyo, Japan). For 3 days, animals were acclimated to treadmill running for 5 minutes at a speed of 10 m/min on a 0% grade. After the acclimation, animals ran on a treadmill with a 10% uphill grade starting at a speed of 10 m/min for 5 minutes. Every subsequent 2 minutes, the speed was increased by 2 m/min until the mice were exhausted. Exhaustion was defined as the inability of the animal to remain on the treadmill despite mechanical prodding. Running time and speed were measured, and the distance was calculated. Grip strength was measured using a MK-380M grip strength meter (Muromachi Kikai Co., Ltd). The grip strength of each individual mouse was measured 10 times, the same measurements were repeated on the next day, and the highest value of each experiment was used.

Statistics

Values were expressed as means ± SD. Statistical significance was assessed by Student's *t*-test. In comparisons of more than two groups, nonrepeated measures analysis of variance (analysis of variance) followed by the Student-Newman-Keuls test were used. A probability of less than 5% ($P < 0.05$) or 1% ($P < 0.01$) was considered statistically significant.

Results

Genetic Differences in Skeletal Muscle Regeneration

To examine the long-term regeneration ability of four inbred strains of mice, repeated cycles of degeneration–regeneration were induced by injection of cardiotoxin (CTX). CTX was injected into one side of the tibialis anterior (TA), gastrocnemius (GC), and quadriceps (Qu) muscle every 2 weeks. At the last (sixth) CTX injection, another intact TA muscle received CTX once to examine the regenerative potential in one cycle of each mouse at this age. Four weeks later, the muscles were removed and analyzed. As shown in Figure 1, A and B, none of the strains displayed a striking difference in either skeletal muscle weight or histochemistry after one CTX injection (CTX-1), except for the appearance of adipocytes in BALB/c. However, the DBA/2 mice that received six CTX injections (CTX-6) exhibited remarkably impaired regeneration (Figure 1A) and loss of TA muscle weight (Figure 1B). A similar loss of muscle weight was also observed in GC and Qu of DBA/2 (CTX-6 in Figure 1C). In contrast, none of the other strains showed a significant difference in uninjured muscle weight at this age (uninjured in Figure 1C). Fat was observed in DBA/2, BALB/c, and C3H/HeN after six injections, but the sclerosis and loss of muscle weight was remarkable in DBA/2. Therefore, the following experiments were performed on C57BL/6 and DBA/2.

Regeneration Impairment in DBA/2 Is Inherited Recessively

To assess the inheritance of the lower regeneration ability of DBA/2, we injected CTX into C57BL/6, DBA/2, and their F1 mice (B6D2F1). To allow more sufficient regeneration time, the interval between CTX injections was changed to 4 weeks. As shown in Figure 2A, we found marked muscle weight loss in DBA/2 after three CTX injections (4 weeks × 3). The results of B6D2F1 mice were similar to those of C57BL/6 (Figure 2, A and B).

As shown in Figure 1A, DBA/2 mice exhibited impaired regeneration accompanied by accumulation of fat and fibrosis after three CTX injections (4 weeks × 3), but not in the 4 weeks × 1 experiment (Figure 2B). Oil red-O (Figure 2C) and Sirius Red (Figure 2D) stainings were performed to determine the amount of fat and fibrosis, respectively. As shown in Figure 2E, increments in fat and fibrotic areas were observed in DBA/2 mice receiving

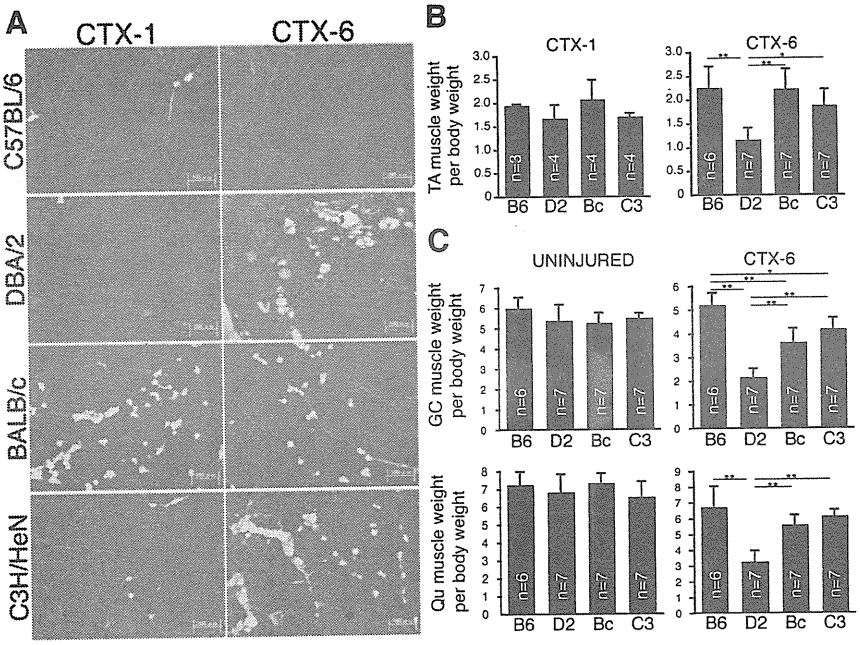

Figure 1. Impaired regeneration and loss of muscle weight in DBA/2 mice after injured six times. **A:** TA (tibialis anterior) muscles were examined histologically in four inbred strains of mice after one (CTX-1) or six (CTX-6) cardiotoxin (CTX) injections. The cross sections were stained with H&E. Scale bar = 100 μm. **B:** The TA muscle weight (mg) per body weight (g) in each inbred strain after one or six CTX injections. B6, D2, Bc, and C3 indicate C57BL/6, DBA/2, BALB/c, and C3H/HeN mice, respectively. **C:** The GC (gastrocnemius) and Qu (quadriceps) muscle weights (mg) per body weight (g) in each inbred strain from uninjured or muscle injured six times. The number in the each graph indicates the number of mice used in these experiments. $^{*}P < 0.05$, $^{**}P < 0.01$ (analysis of variance, SNK-test).

three injections (4 weeks × 3). In 4 weeks × 1 DBA/2, the fat accumulation of one mouse was a slightly higher volume (2.02%), but three mice showed little fat accumulation (less than 0.6%). In contrast to DBA/2, C57BL/6, and B6D2F1 mice did not show any sign of impaired regeneration. These results indicate that the impaired regeneration ability of the DBA/2 strain after repeated injury is recessive heredity.

Loss of Muscle Mass Results from Decreased Number and Size of Myofibers

To assess the cause of muscle weight loss in DBA/2, the numbers and sizes of myofibers were quantified. In uninjured muscle, no significant difference between the numbers of myofibers was observed in C57BL/6 and DBA/2 (Figure 3A). However, as shown in Figure 3B, decreased numbers of myofibers were observed in DBA/2 after three CTX injections (4 weeks × 3), as compared with 4 weeks × 1 or uninjured muscle. C57BL/6 showed more myofibers than uninjured muscle after one or three injections (Figure 3B).

The sizes of myofibers were also measured. Four weeks after one CTX injection (4 weeks × 1), the size of myofibers in DBA/2 was similar to that in C57BL/6 (Figure 3, C and D). However, the regenerated myofibers of DBA/2 (4 weeks × 3) were slightly smaller than those of C57BL/6 (Figure 3, C and D). These data indicate that the loss of muscle weight in DBA/2 results from the decreased number and size of myofibers.

Decreased Number of Self-Renewed Satellite Cells in DBA/2

We hypothesized that a decreased number of satellite cells leads to the loss of myofibers, because myofibers are mainly made by satellite cells. To elucidate this hypothesis, we examined the number of satellite cells. As shown in Figure 3E, cells positive for Pax7, a specific marker of satellite cells,[21] lying beneath the basal lamina were counted. There was no significant difference between the uninjured TA muscles of C57BL/6 and DBA/2 mice. However, a remarkable decrease in the number of satellite cells was observed in DBA/2 after three CTX injections (Figure 3F). These results imply that the functions (including self-renewal potential) of satellite cells include responsibility for most of the regeneration of impaired muscle in DBA/2.

Colony Formation and Proliferation of Satellite Cells from DBA/2

To examine whether there is an intrinsic difference between the satellite cells of C57BL/6 and DBA/2, satellite cells were isolated and cultured *in vitro*. As shown in Figure 4A, the BrdU uptake of primary myoblasts of DBA/2 was inferior to that of C57BL/6 myoblasts. Next, we performed a colony-forming assay of single satellite cells. As shown in Figure 4C, single DBA/2 satellite cell did not produce large colonies similar to those of C57BL/6. The frequencies of colony forming cells did not differ in C57BL/6 and DBA/2 (Figure 4B). These results indicate that intrinsic factors affect the properties of satellite cells.

Loss of Muscle Weight in DBA/2-mdx

To assess whether the low regenerative potential of mice with the dystrophin mutation exhibit DMD-like features, we crossed C57BL/10-*mdx* (B10-*mdx*) into DBA2. It was reported that body weight of B10-*mdx* is heavier than that of the control wild-type.[22] In contrast to B10-*mdx*, DBA/

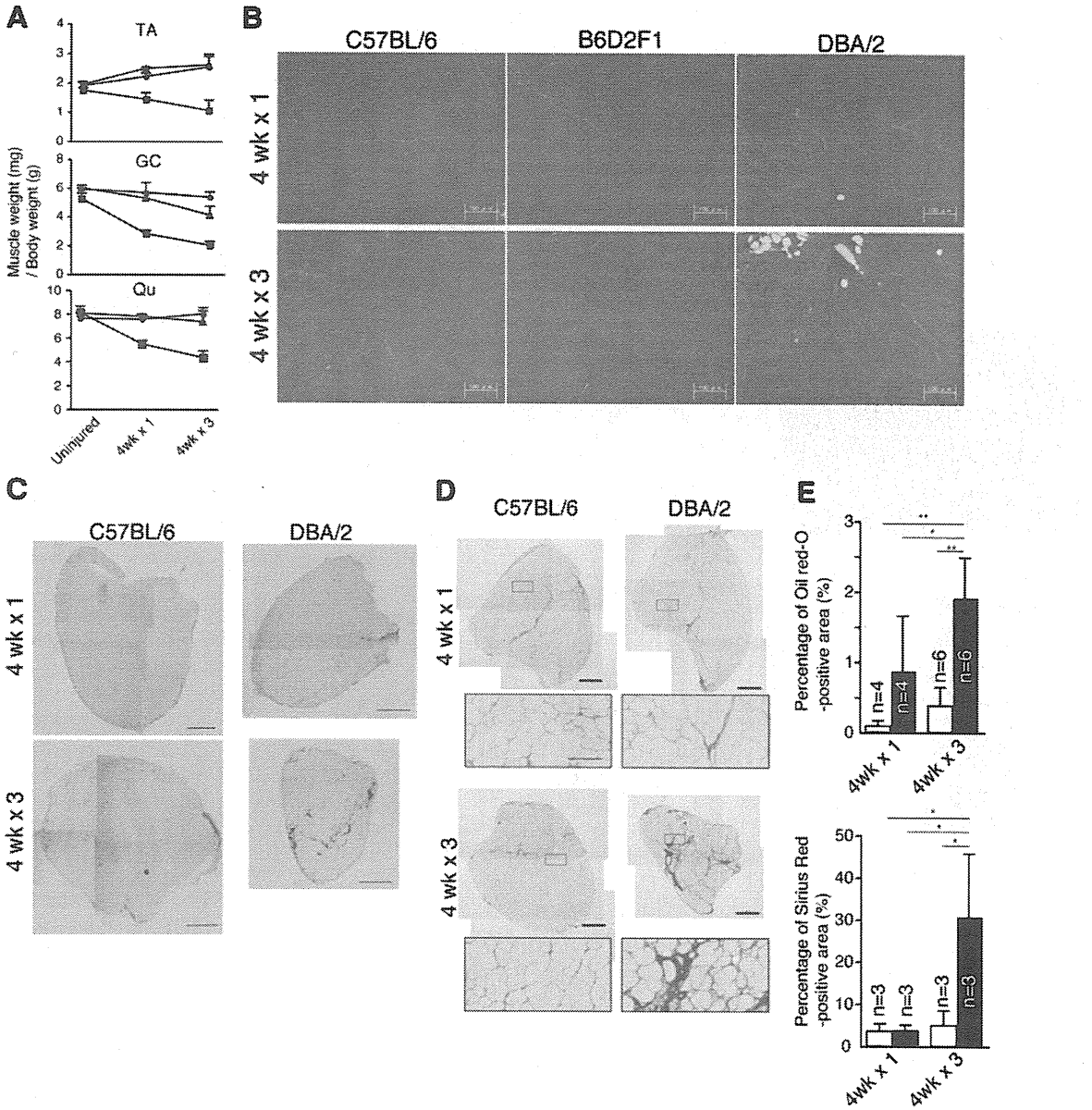

Figure 2. Impaired regeneration of DBA/2 phenotype is recessively inherited. **A:** The TA, GC, and Qu muscle weights (mg) per body weight (g) in C57BL/6 (closed circles), DBA/2 (closed squares), and B6D2F1 (closed triangles) mice after one (4 weeks × 1) or three CTX injections (4 weeks × 3). The cross sections were stained with H&E (**B**), Oil red-O (**C**), or Sirius Red (**D**). Scale bars: 100 μm (**B**); 500 μm (**C** and **D**). **E:** The *y* axis shows the mean percentage of Oil red-O or Sirius Red-positive areas per section. White and black columns indicate the results of C57BL/6 and DBA/2, respectively. The number in the each graph indicates the number of mice used in this analysis. $^{*}P < 0.05$, $^{**}P < 0.01$ (analysis of variance, SNK-test).

2-*mdx* (D2-*mdx*) mice showed the decreased body weight regardless of gender (Figure 5A). A more remarkable phenotype of D2-*mdx* was the loss of skeletal muscle mass (Figure 5B). As previously reported, the muscle weight of B10-*mdx* was heavier than that of controls,[8] but the TA, GC, and Qu muscle weights of D2-*mdx* males were 71%, 59%, and 54% of those of controls, respectively (Figure 5C). Female muscles were 85% (TA), 61% (GC), and 52% (Qu) of each control muscle, respectively. The loss of muscle weight did not simply reflect the decreased body weight because there is also a significant difference in muscle weight (mg) per body weight (g) between D2-*mdx* and control littermates (Figure 5C). Control littermates of D2-*mdx* and normal DBA/2 exhibited similar results in muscle weight per body weight ratios (data not shown).

Histology of DBA/2-mdx

In contrast to the histology of DMD, it is widely accepted that fibrosis and fat replacement are minimal in B10-*mdx*.[7] In addition, there was no apparent fiber loss. To examine the accumulation of fibrosis and fat tissue in D2-*mdx*, cross sections were stained with Sirius Red or Oil red-O. As shown in Figure 6, A and B, there was no sign of fibrosis or adipogenesis in B10-*mdx*. However, D2-*mdx* mice exhibited increased fibrosis and fat accu-

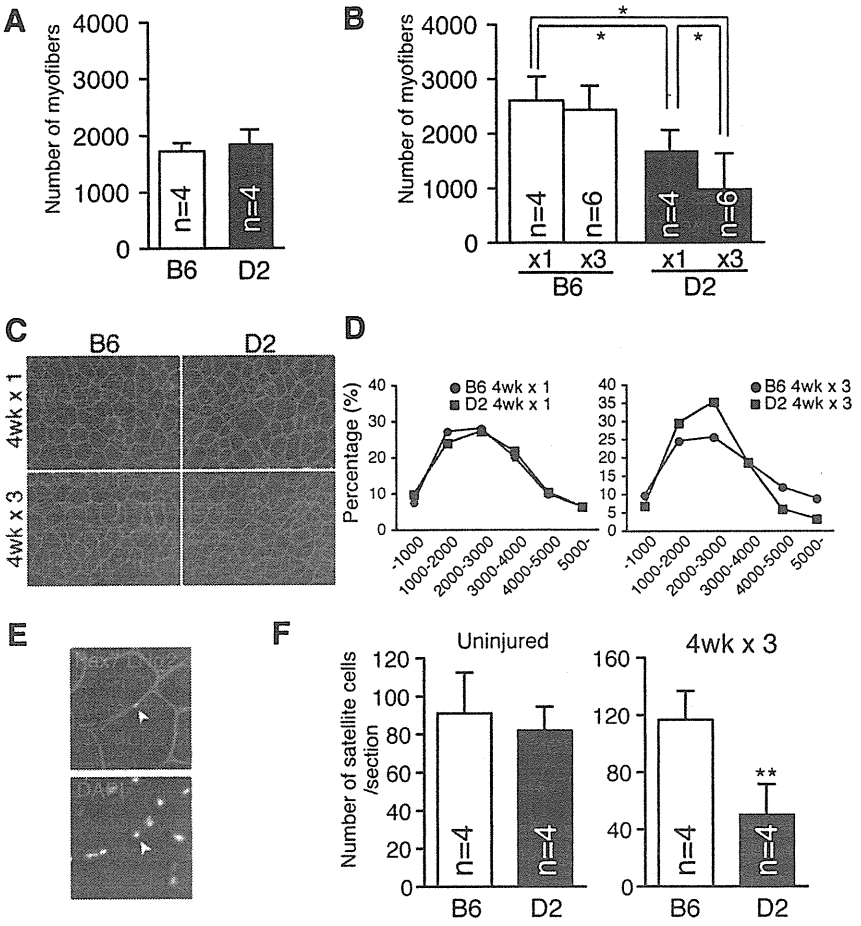

Figure 3. Decreased numbers of myofibers and satellite cells in DBA/2 mice after three repeated injuries. **A:** The number of myofibers in uninjured TA muscle at 10 weeks old. The *y* axis shows the mean number of myofibers per section. B6 and D2 indicate C57BL/6 and DBA/2, respectively. **B:** The mean numbers of myofiber in TA muscles after one or three injuries. $^{*}P < 0.05$ (analysis of variance, SNK-test). The sizes of myofibers in TA muscle after one or three CTX injections. **C:** Cross sections were stained with anti-laminin α2 antibody (green). **D:** The size of each myofiber in TA muscle was measured after one or three injections. Closed circles or squares show the results of C57BL/6 or DBA/2, respectively. **E: Arrowhead** indicates Pax7 expressing cells lying beneath the basal lamina. **F:** The number of satellite cells in noninjured TA muscle (uninjured) or TA muscle injured three times (4 weeks × 3). The *y* axis shows the mean number of satellite cells per section. The number in each graph indicates the number of mice used in these analyses. $^{**}P < 0.01$ (Student's *t*-test).

mulation in comparison with B10-*mdx*. In contrast to B10-*mdx*, a decreased number of total myofibers was also observed in D2-*mdx* (Figure 6C).

To enumerate the number of necrotic fibers, the mice were injected with Evans blue dye to visualize necrotic fibers. As shown in Figure 6C, fewer total necrotic fibers were observed in D2-*mdx*. This result suggests that the D2-*mdx* phenotype does not result from acceleration of degeneration.

*Decreased Skeletal Muscle Function in DBA/2-*mdx

Skeletal muscle endurance was assessed by treadmill running to exhaustion as an indicator of maximal muscle capacity. After acclimatization, mice were run on a 10% slope at increasing speed until the animals were unable to remain on the treadmill despite prodding. We then recorded the end time and speed to calculate the distance run. As shown in Figure 7A, male and female D2-*mdx* ran 45% and 56% shorter distances than control littermates. The maximum speed of D2-*mdx* was also lower than that of their littermate. The distance run showed the most significantly difference because of the protocol of increasing speed (Figure 7A). The average distance run by male controls was 544 meters, but that of D2-*mdx* males was 205 meters (38% of the control). A similar result was shown by female D2-*mdx* (25% of the control). B10-*mdx* also showed lower values compared with normal C57BL/10 mice (data not shown), but the decreased ratio of each parameter in D2-*mdx* was more remarkable than that in B10-*mdx* (Figure 7B).

A grip strength test was also performed as an indicator of motor function and whether D2-*mdx* exhibited muscle weakness compared with controls. As shown in Figure 7C, D2-*mdx* earned a lower score than control mice regardless of gender. However, there was no significant difference between B10-*mdx* and control mice.

Discussion

Repeated Injury Models

Muscle satellite cells play central roles in skeletal muscle regeneration.[23] Satellite cells produce a vast number of progenitor cells (myoblasts) that finally become myofibers. During this process, at least some of the satellite cells have self-renewal potential,[14,24] but are quiescent and will respond efficiently to the next damages. In fact, Luz et al[15] indicated that C57BL/10 could regenerate after 50 bupivacaine injections without the loss of myofibers or gain of fibrotic areas in the TA muscle. Importantly, C57BL/10-*mdx* mice exhibited decreased numbers of myofibers after 50 bupivacaine injections[15]